Table of Contents

1. Summary

This project ultimately investigated the effect of MgO additive on oil well cement's resistance to CO_2 degradation. A patented CO_2 resistant cement was also tested to try to verify its effectiveness and provide useful comparison.

Cement samples were made with varying amounts of MgO additive (up to 6% MgO content by weight). Four different experiments were performed to simulate and accelerate the effect of CO_2 degradation. Only one of these simulations was successful at replicating known effects of CO_2 degradation on oil well cement. Increased addition of MgO did not prevent the effects of CO_2 degradation nor did it cause a noticeable decrease in the rate of degradation.

MgO, alone or in the presence of Portland cement, hydrates to form magnesium hydroxide (Brucite – $Mg(OH)_2$), which is generally weak, and in the presence of CO_2 would carbonate to form one or more of a range of hydrated magnesium carbonates, which are generally strong. Both reactions are expansive and could lead to densification of the microstructure and hence enhanced strength.

In this study the curing processes adopted in cement manufacture were similar to that recommended by the American Petroleum Institute (API) Specifications for simulating the oil well cementing process. Crucially this curing process did not cause additional Brucite to form as a hydration product as MgO addition was increased. Portlandite underwent carbonation regardless of MgO addition but there was no evidence of Brucite carbonation taking place.

The results of testing the patented CO_2 resistant cement against CO_2 degradation were inconclusive. It is clear that the chemical composition of this cement is very different and more work will be required to identify possible degradation mechanisms and whether they exist.

2. Background and Motivation for Study

Two major Engineering initiatives are likely to play a big role in the future with the sustainability of oil production and greenhouse gas emissions being brought into question;

- Carbon Capture Sequestration (CCS)
- Gas injection Enhanced Oil Recovery (EOR)

The success and reliability of these methods is highly dependent on having cements that are resistant to degradation upon exposure to CO_2.

2.1 CCS

CCS involves injecting CO_2 into geological formations such as saline aquifers and disused oil fields with a view to long term storage. If this can be done successfully then the effect of atmospheric CO_2 emissions can be mitigated.

The UK government alone has set aside a £1billion fund to further the development of CCS technologies in recognising the potential of CCS to abate CO_2 emissions. [1a]

CCS presents many technological challenges, including separating the CO_2 from the flue gases, transporting the CO_2 to the injection site and injection to a suitable sub-surface site. For CCS to be viable the stored CO_2 must not be allowed to leak for at least 1000 years. Over this timescale it should be possible to account for 99% of CO_2 injected. [1]

2.2 Gas Injection EOR

Gas Injection EOR is a procedure used to increase the amount of oil recovered (the Recovery Factor – RF) from an oil field or reservoir. The RF is broadly defined as;

$$\text{RF} = \frac{Actual\ Amount\ of\ Oil\ Recovered\ from\ field\ (STP)}{Standard\ Tank\ Oil\ Initially\ In\ Place\ (STOIIP)}$$

By injecting gases such as CO_2 into a depleted reservoir the field's energy is increased and the well can carry on producing for longer. Increasing the Gas-to-Oil ratio of the reservoir fluid also serves to reduce its viscosity and reduce hydrostatic pressure losses in the production well (average density of the fluid is lower). These factors also contribute to an increased Recovery Factor.

While Gas Injection EOR does not mitigate CO_2 emissions in the same way as CCS it nevertheless has a big role to play in reducing the environmental impact of oil production and exploration and increasing the industry's sustainability. As oil prices continue to rise it is likely to become more economically favourable. [2]

2.3 CCS and oil producing wells in the same geological area

Sites that are attractive for CCS (e.g. Saline aquifers, abandoned oil and gas fields) are often in the same area as pre-existing oil production and injection wells. In well-exploited fields the number of wells can be large and given that recent studies have shown leakage rates of up to 4.6% (a study of 316,000 wells analysed in Alberta, Canada[1]) there may well exist artificial

pathways for leakage to occur. It is vital that these issues are addressed before any site is used for CCS.

3. Leakage Mechanisms and Cement types

Once injected into the subsurface the plume of CO_2 may move upwards or sideways due to buoyancy effects and pressure differences.

Inevitably any injection wells drilled into a natural formation present an obvious pathway for leakage to occur.

It is vital that the integrity of the well bore is maintained for the required timescale in order for CCS to be feasible.

There are several possible ways CO_2 can leak through a well (Figure 3.1). They include the steel casing cement interface and cement plug steel casing. The scope of potential leakage paths is very large but it is clear that any degradation in the physical properties of cement will compromise the integrity of the well.

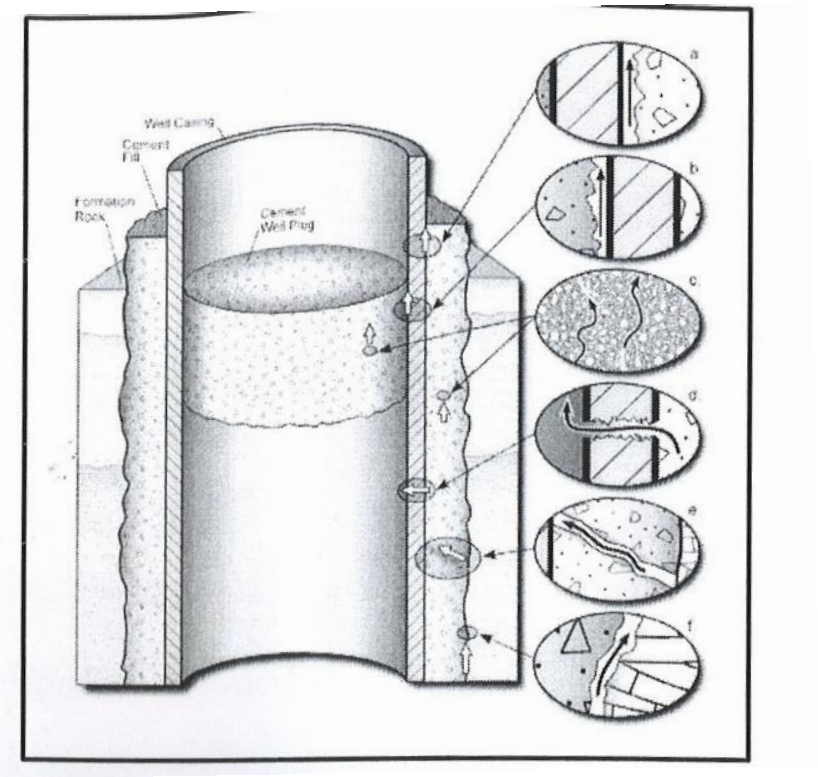

Figure 3.1 – Potential leakage paths for CO_2 to escape through well[1]

4. Conditions encountered in Well Bore

Cement used may have to withstand the following harsh conditions. Research is still very much active in trying to find cements suited to this purpose.

- High CO_2 concentrations (up to 22%)
- High Temperatures (up to 350°C)[5]
- High Salinity Environments
- High Pressures (up to 200MPa)[5]
- pH – CO_2 dissolves in water to form Carbonic Acid.
- Mechanical Factors e.g. thermal cycles caused by choking and opening of the wells leading top large temperature variations.
- High sulphur environments.

There is clearly huge scope for investigating how cement performance varies with typical well bore conditions.

5. Cement used in Well Construction

Oil well cement is based on Portland Cement and consists of a clinker material made up of Calcium Silicates, Iron and Aluminium compounds These tend to be used most in current drilling operations and it is a good starting point for our investigation.

Oil well cements are classified (by the American Petroleum Institute – API) depending on their suitability for different temperature and pressure ranges (which often translates to the depth they can be used at) along with their Sulphate resistance. They are classified as types A-H.

Classes G and H are the most commonly used types in the petroleum industry. Many additives are often added depending on the conditions the well will be likely to encounter. The scope of additives used is very large and there is no standard cement mixture. Well Cementing by Schlumberger [3] provides more detailed reading about additive effects but is by no means an algorithm to follow when drilling a well. A non-exhaustive summary of common additives is given below;

- Density Reduction/Weight Materials
    - The density of well cement is crucial depending on the pressures encountered in drilling and to ensure fracturing does not occur.
    - Benonite, pozzolans and nitrogen are used to reduce cement density.
    - Barite, hematite and sand are commonly used as weight materials.
- Viscosifiers are needed to increase the cement's flowability when it is pumped downwards during drilling e.g. NaCl and Calcium Lignosulphate.

- Filtration control additives to prevent the cement slurry leaking into porous and permeable formations e.g. $Ca(OH)_{2\ (aq)}$ or Caustic Soda.
- Accelerators and Retarders control the time taken for the cement to harden or set (the point at which the cement develops strength and becomes impermeable to fluids). Calcium, Sodium and Potassium Chloride are all used as accelerators while Calcium and Lignosulfate and other organic compounds such as cellulose can be used as retarders.

6. Typical Theoretical Degradation process Mechanism

The cement sheath in the well bore is the first material that the injected CO_2 encounters. Often in CO_2 rich environments cements will undergo carbonation. Carbonation can have a marked effect on the cement's physical properties.

Now oil well cement is a Portland cement derivative and its main hydration products can be considered to be Calcium Silicate Hydrate (CSH, $Ca_2Si_2O_7\ .4H_20$) and Portlandite ($Ca(OH)_2$).

CO_2 dissolves in water to form Carbonic Acid. Carbonic Acid's pH can be as low as 2.9[5]

$$CO_2 + H_2O \Rightarrow H_2CO_{3(aq)}$$

The porewater in the cement around the Portlandite will be highly alkaline with a pH potentially as high as 12.3[5]. The Carbonic Acid diffuses into the porous cement matrix and the imbalance in pH drives the reaction which dissolves the Portlandite;

$$Ca(OH)_{2(s)} \Rightarrow Ca^{2+}{}_{(aq)} + 2OH^-{}_{(aq)}$$

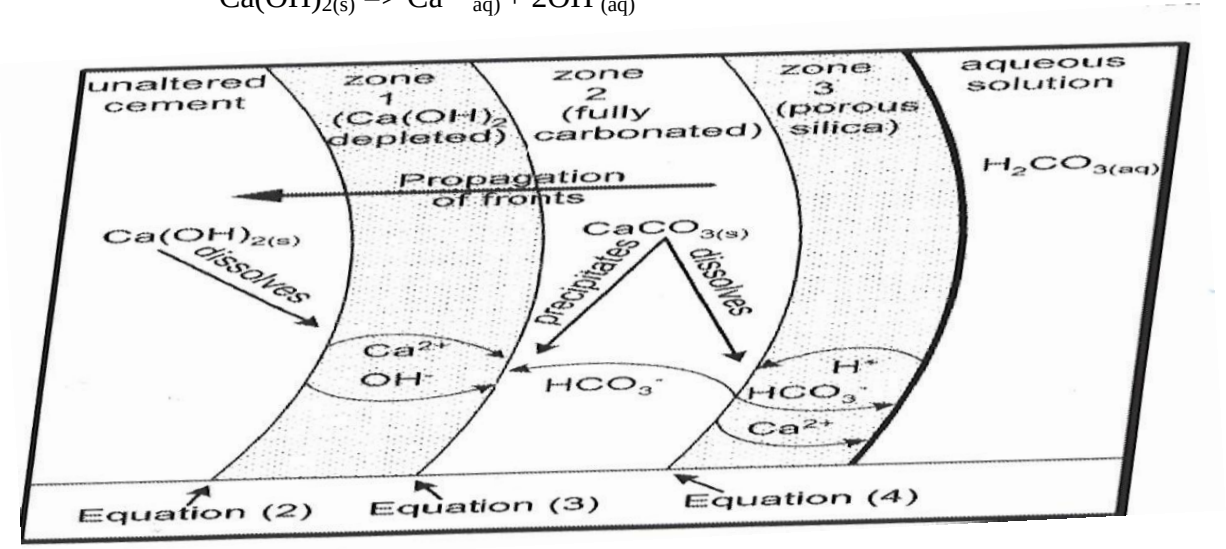

Figure 6.1 – Degradation fronts as a result of cement carbonation[5]

This translates to Zone 1 on the figure where Portlandite is dissolved and depleted. This leads to a slight reduction in porosity.

As the porewater in the cement matrix reacts with the Carbonic Acid it's pH falls. This means more CO_2 dissolves and more CO_3^{2-} is present. This reacts with the Portlandite to precipitate out $CaCO_3$ (Calcite):

$$Ca(OH)_2 + CO_3^{2-} + 2H^+ = CaCO_3\ (s) + 2H_2O$$

This reaction corresponds to Zone 2 in the figure and is actually a self-healing reaction that improves the cements properties. The higher proportion of $CaCO_3$ present lends to increased strength and the higher molar volume (compared with the Portlandite) reduces the cement's porosity.

Inevitably the reaction does not stop here and the cement in Zones 3 has less desirable properties. As the $Ca(OH)_2$ is depleted the pH buffering action is reduced. This drop in pH means that more CaCO3 dissolves, leading to more bicarbonate (HCO_3^-) production;

$$H^+_{(aq)} + CaCO_3 => Ca^{2+}_{(aq)} + HCO_3^-{}_{(aq)}$$

The bicarbonate ions produced are water soluble and can diffuse of the cement matrix. As the $CaCO_3$ is used up the cement loses the ability to buffer the pH. This pH drop causes the remaining Calcium Silicate Hydrates (C-S-H) to react with the Carbonic Acid forming amorphous Silica gel (SiO_2*H_20 in the reaction below).

$$3H_2CO_3 + Ca_3Si_2O_7.4H_2O => 3CaCO_3 + 2SiO_2.H_2O + 3H_2O$$

$SiO_2.H_2O$ has a higher molar volume than $CaCO_3$ so the porosity of the cement in Zone 3 is higher. SiO_2*H_20 also lacks structure and the strength of the cement here is much lower.

In spite of the current high levels of use of Class G and Class H cements they are not designed to be CO_2 resistant. This project will attempt to observe some of this predicted degradation and make suggestions for eliminating/reducing it.

7. Effect of MgO as an additive in cement

Studies by Liska et al. [6,7] have suggested that adding reactive MgO as an additive to cement lends to increased strength and toughness after undergoing carbonation. This is because Brucite can form as a hydration product in MgO based cements by the following reaction:

$$MgO + H_2O => Mg(OH)_2$$

If Brucite undergoes carbonation (which is hoped to be the case in a CO_2 rich environment) products such as Nesquehonite ($MgCO_3(H_2O)_3$), Dypingite ($Mg_5(CO_3)_4)(OH)_2.5H_2O$) and Hydromagnesite ($Mg_5(CO_3)_4)(OH)_2.4H_2O$), which are very beneficial to the cement's microstructure, are formed by the following reactions:

Nesquehonite: $Mg(OH)_2 + CO_2 + 2H_2O \Rightarrow MgCO_3.3H_2O$

Dypingite: $Mg(OH)_2 + 4CO_2 + 5H_2O \Rightarrow Mg_5(CO_3)_4)(OH)_2.5H_2O$

Hydromagnesite: $Mg(OH)_2 + 4CO_2 + 4H_2O \Rightarrow Mg_5(CO_3)_4)(OH)_2.4H_2O$

After reading literature about using MgO as an additive this seems a logical investigation pathway to follow given the desired outcome.

8. Challenges of the Project

Section 4 highlighted the extreme conditions that can be encountered around the well bore. Replicating such high temperatures and pressures in the lab can often be impractical and also presents various safety considerations.

Even in such extreme conditions the degradation process can be very slow evolving over many years. Indeed many studies already undertaken in this field sometimes involve experiments lasting several years.

An unavoidable constraint of the 4th Year project is that results must be collected by the end of March i.e. within 6 months. As such techniques which attempt to accelerate this degradation process should be used wherever possible.

8.1 Accelerated CO_2 degradation process – LIFTCO2 Procedure

A study by Rimmelé and Gouedard[8] used the set-up in Figure 8.1.1 to accelerate the CO_2 degradation process by applying a potential difference (of up to 30V) and inducing a process called electrophoresisis (leaching causes forced transport of the cement ionic species). CO_2 is bubbled through both sides of the tank at 100ml/min and the cement is held in a Perspex sample holder sealed to the tank.

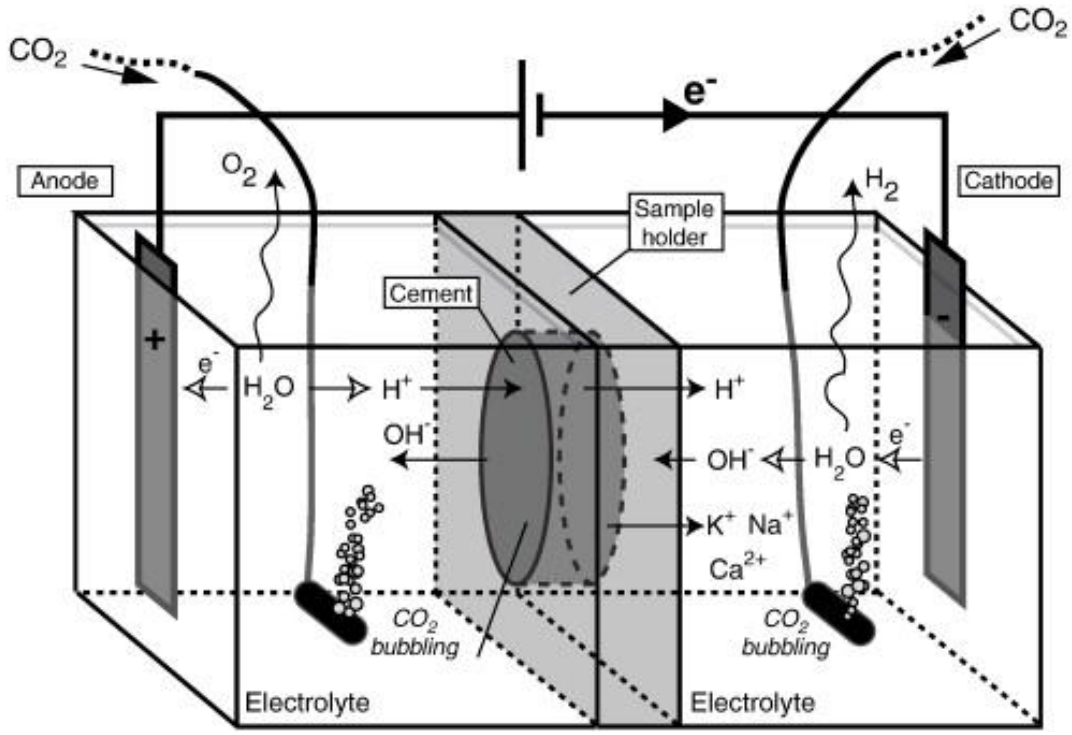

Figure 8.1.1 – The LIFTCO2 cell[8.1]

8.2 Observing Degradation Process

Degradation can often be small requiring reliable apparatus to observe experimentally:

- Hydraulic Testing Machine. Measures Ultimate Compressive Strength (UCS) by testing the cement samples to destruction.
- Mercury Intrusion Porosity Evaluation (MIIP). Technique is very expensive and so was not used.
- Electron Scanning Microscope (ESM). Can be used to observe changes in microstructure by providing magnifications potentially up to x500,000. ESM's are expensive to use so for this 4th year project use is limited to 3-4 hours. As such it is important to be selective as to which samples are sent for ESM analysis.
- X-Ray Diffraction (XRD). By observing the scattering intensity of an incident x-ray beam on the cement the presence of hydration products can be verified. This can be done in the form of detailed quantitative analysis by integrating areas under the peaks by the Reference Intensity Ratio Method (RIR). A standard phase of known proportion can be introduced from which to deduce compositions.[13]
- Permeameters. Can be used to estimate sample permeabilities by either measuring the time for penetration (for low permeabilities) or penetration rate (for high permeabilities) of fluid through a cement sample when driven at pressure. The

permeability of the cements tested is extremely low and preliminary experiments showed negligible flows of water through cement samples even after 2 weeks. As such this method was not used further.

9. Experimental Procedures

Section 5 highlighted the vast range of additives typically used in well cementing. It is likely that any cements used for CCS would also be of very complex compositions.

In order to make logical and valid conclusions it is important to keep any experiments as simple as possible. Solely MgO (Grade: 94/200 supplier: Richard Baker Harrison) shall be used as an additive in our investigations and its composition varied. Delayed hydration of Periclase (a cubic form of MgO) causes long term expansion if too much additive is used so in practice this is normally limited to a 6% addition.[4]

In order to undertake the investigations two different sized samples were made:

1) Large samples were fabricated using cylindrical plastic moulds of 100mm height and 50mm diameter.
2) Smaller cylindrical samples of 12.5mm diameter and 20mm height. The moulds took the form of 40 12.5mm diameter holes drilled in a Perspex sheet.

9.1 Preparation of samples

Clingfilm and sellotape were used to seal the bottom end of the mould to make the large samples.

Samples were made up of 3 different compositions as follows:

Table 9.1.1 - Cement compositions investigated

Composition (by Weight)	API Class G Cement	Water	MgO (Grade 94/200)
Mixture 1	100	44	0
Mixture 2	100	47	3
Mixture 3	100	50	6

The cement was supplied by Cebo UK, Great Yarmouth. It's chemical composition is given in Table 9.1.2 (More detailed data sheet in Appendix).

Table 9.1.2 – Composition of API Class G Cement

Component	**Percentage (%)**
MgO	1.8
SO_3	2.6
C_3A	2.2
$C_4AF + 2C_3A$	17.3
C_3S	57.0
$(0.658xK_2O) + Na_2O$	0.5

Abbreviations C-CaO, S-SiO_2, A-Al_2O_3,F-Fe_2O_3

Batches of approximately 8-10 samples were made for each mixture. A mass balance (figure 9.1.1) was used to first ensure the correct proportion of mixture constituents were added to a metal bowl.

Thorough mixing of each batch then took place for approximately 10-15 minutes to try to ensure homogenous properties throughout all the samples. A food mixer (figure 9.1.2) was used for several minutes at a time interspersed with manual mixing with a metal spatula to prevent build up off thicker cement along the bowl walls and improve the quality of mixing.

Figures 9.1.1 and 9.1.2: Mass balance and food mixer

The compositions investigated are somewhat arbitrary. For a mixture of solely water and cement the API recommendation of a water cement ratio of 44% has been taken. With addition of MgO additive the water composition is increased to try to ensure similar flowability's of the mixture. It turns out that the compositions in table 9.1.3 do this as

indicated by the time to pour 3kg of cement mixture from one metal bowl to another (time stopped when flow rate is no longer appreciable – some cement will stick to the initial bowl)

Table 9.1.3 Time (s) to pour 3kg of mixture

Mixture 1	9.5
Mixture 2	10.1
Mixture 3	9.8

This rather rough and ready approach shows that the mixtures investigated have similar viscosities and thus are similar to what would be required in well cementing applications.

After mixing took place the samples were poured into their respective moulds and left to set for 24 hours at ambient conditions in the lab (figures 9.1.3 and 9.1.4). They are then removed from their moulds and placed in a water bath at 60°C for 24 hours to cure in a manner similar to the API Specifications.The curing process used is suitable for our study as any injection wells drilled for the purposes of CCS will likely be of a similar design to producing oil wells.

Figure 9.1.3 (left): Leaving small samples to set – thick residue on top can be scraped off. Figure 9.1.4 (right): A large sample setting

In addition to investigating API Class G Cement and MgO mixtures a patented CO_2 resistant cement was tested.

Confidentiality rules mean that the composition of the CO_2 resistant cement is not known. Only the cement powder was obtained so we were unable to test the actual cement including additives.

The cement powder has a much more sandy and crumbly texture than the API Class G cement. This means that a much lower water: cement ratio of 0.3 is used to obtain a similar

flowability to the Class G cement samples. This water cement ratio takes 9 seconds to pour as per the test in Table 9.1.3.

9.2 Simulating the effect of CO_2 degradation on Cement samples

After curing to replicate the well cementing process, a variety of different simulations have been postulated to try to replicate the effects of CO_2 degradation.

9.2.1 No degradation

Samples are tested without subjecting them to any intentional degradation process. This serves as a control experiment with which to compare with degradation simulations. It is important that all comparisons are made across samples of the same age so once cured the samples are stored submerged under water until tested.

9.2.2 Degradation Simulation 1

In this simulation the cement mixture is made with weakly Carbonic Acid as opposed to water to try to encourage products of Carbonation to form upon hydration of the cement.

The weakly Carbonic Acid is obtained by bubbling CO_2 through a bucket (approximate size of 5 litres) of cold water for 24 hours at approximately 200ml/min, adding ice periodically to keep the temperature close to 0°C.

The reason for keeping the temperature low is to increase the solubility of CO_2 in the water. Figure 9.2.2.1 shows solubility at 0°C to be approximately double that at 20°C – a plausible estimate of ambient temperature.

The relative increase in solubility of the CO_2 in the water seems to be confirmed by taking readings of the pH periodically and until it reaches a steady value after a few hours. Figure 9.2.2.2 highlights how pH reaches an equilibrium value after bubbling CO_2 through the water for a few hours.

The samples are then set and cured in an identical manner to the control process. After curing the samples are stored under water at ambient conditions until ready for testing.

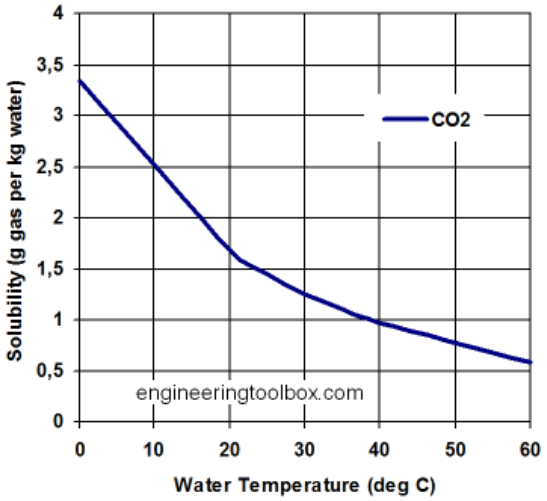

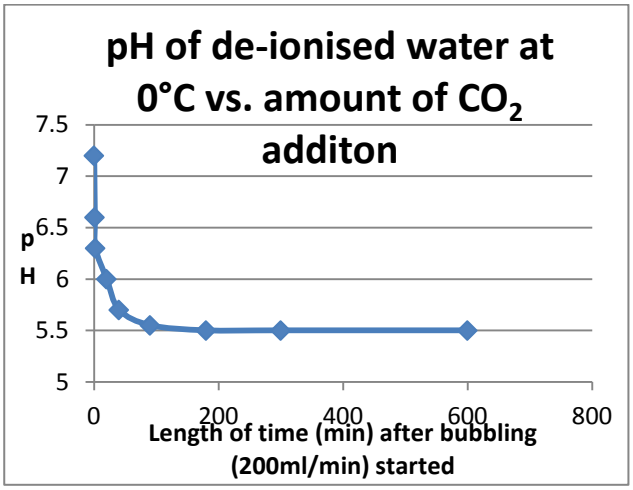

Figure 9.2.2.1 (right): fall in pH of de-ionised water with CO_2 addition. Figure 9.2.2.2 (left): Solubility of CO_2 in Water vs. Temperature

9.2.3 Degradation Simulation 2

The samples are mixed, set and cured in the same way as the control process (see Section 9.2.1). Then the samples are left to soak in Carbonic Acid for 1 week. CO_2 is continually bubbled through the water at 200ml/min while ice is periodically added for the first day to keep the temperature close to 0°C and maximise CO_2 dissolution.

After 1 week of soaking the cement samples in the Carbonic Acid they are removed, wrapped in a breather blanket (Figures 9.2.3.1 and 9.2.3.2) , bagged and sealed using high temperature film and tape (the samples are wrapped and sealed while still damp to increase the amount of Carbonic Acid present in the sealed bag). A vacuum port is placed on the outside of the film. Figures 9.2.3.3 and 9.2.3.4 illustrate this.

The vacuum port is attached to the pump and a vaccum created (Figure 9.2.3.5). The vacuum is necessary to prevent overly high pressures occurring at high temperatures which might lead to explosions if the structural limitations of the film and tape are exceeded. The bag and its contents are placed in the structures lab oven and left for 5 hours at 250°C. Care is taken to allow the samples to cool (for at least 2 hours) before removing them from the kiln with gloves.


Figures 9.2.3.1 and 9.2.3.2 – Wrapping the cement samples in breather blanket

It was hoped that the breather blanket would absorb any moisture as this evaporated from the damp samples while sealing and bagging would prevent any of the CO_2 (released as the Carbonic Acid evaporates) escaping. The idea is to create a harsh high temperature, humid and CO_2 rich environment to encourage degradation. Note that a necessary assumption here is to neglect the decrease in solubility of CO_2 in water as the pressure drops.

After cooling the samples are stored under water at ambient conditions until ready for testing.


Figure 9.2.3.3 (above left), 9.2.3.4 (above right) and 9.2.3.5 (below). Sealing the samples, applying vacuum and placing in kiln

9.2.4 Degradation Simulation 3

The samples are mixed as per the previous processes but this time the setting and curing processes take place in a CO_2 rich environment.

After pouring the samples they are placed in the Geotechnical Lab incubator to set at 30°C (the minimum temperature to which the incubator can be set) and 20% CO_2 - concentration for 24 hours. After 24 hours the samples are submerged in containers of weakly Carbonic Acid that has been prepared as in section 9.2.2. The containers are then placed back in the incubator (Figures 9.2.4.1 and 9.2.4.2) and the temperature increased to the maximum value of 80°C – this causes the Carbonic Acid temperature to rise to about 56°C and ensures the curing process takes place at a similar temperature to the other degradation processes only this time in a CO_2 rich environment.

After the curing process is complete the samples are bagged, sealed and roasted by the procedure described in 9.2.3

Once degradation simulations 1-3 have taken place they are all stored under water until ready for strength testing. It is important this is done at the same time for all samples as strength and the composition of hydration products can vary significantly with age.

Figures 9.2.4.1 (left) and 9.2.4.2 (right) - Placing submerged samples in incubator and setting the temperature and CO_2 concentration.

9.2.5 Degradation Simulation 4 - LIFTCO2 Procedure

Given the aforementioned methods of trying to simulate CO_2 degradation are relatively untried and tested the LIFTCO$_2$ method used by Rimmelé and Gouedard shall be used. This has already been proven in accelerating the degradation process.

At the start of Lent Term, a large LIFTCO2 rig was constructed (following preliminary test experiments in Michaelmas with a smaller rig) to enable up to 40 samples to be tested at one time. Owing to practical size constraints of the rig and the likely extent of degradation (Rimmelé and Gouedard found this to be of the order of 100µm) the rig dealt with smaller cylindrical samples of height 20mm and diameter 12.5mm. A rig was created using a Perspex tank (dimensions 50cm length x 35cm height x 17cm width), electrodes connected to a 30V supply, aquarium heaters and a Perspex sheet. An array of 40 holes (8 rows of 5) was drilled into the Perspex sheet. After mixing the different cement compositions they were poured into some of the holes (lubricated with mould release spray) in the sheet (using cling film and sellotape to seal off holes required for different compositions) as described in section 9.1. 13 holes were filled with Mixture 1 and 2 and 14 were filled with Mixture 3 to ensure maximum utilisation of the holes. The cement was left to set for 24 hours and then cured by placing the Perspex sheet in a water bath at 60°C for 24 hours. After setting and curing the Perspex sheet was placed in the middle of the tank and sealed using Silicon sealant to create 2 separate compartments.

Both compartments were filled with distilled water and an aquarium heater was submerged and held in each compartment. The heaters were set to maximum (raises water temperature to 32°C) and electrodes placed in each compartment (using stands, clamps and bosses). The set-up was left for 35 days occasionally (once every 2 or 3 days) topping up with distilled water to keep the cement samples submerged in water.

After 35 days the Perspex sheet was removed - using a Stanley knife to cut it free - and the samples removed (figures 9.2.5.2 and 9.2.5.3) using a hammer and nylon rod.

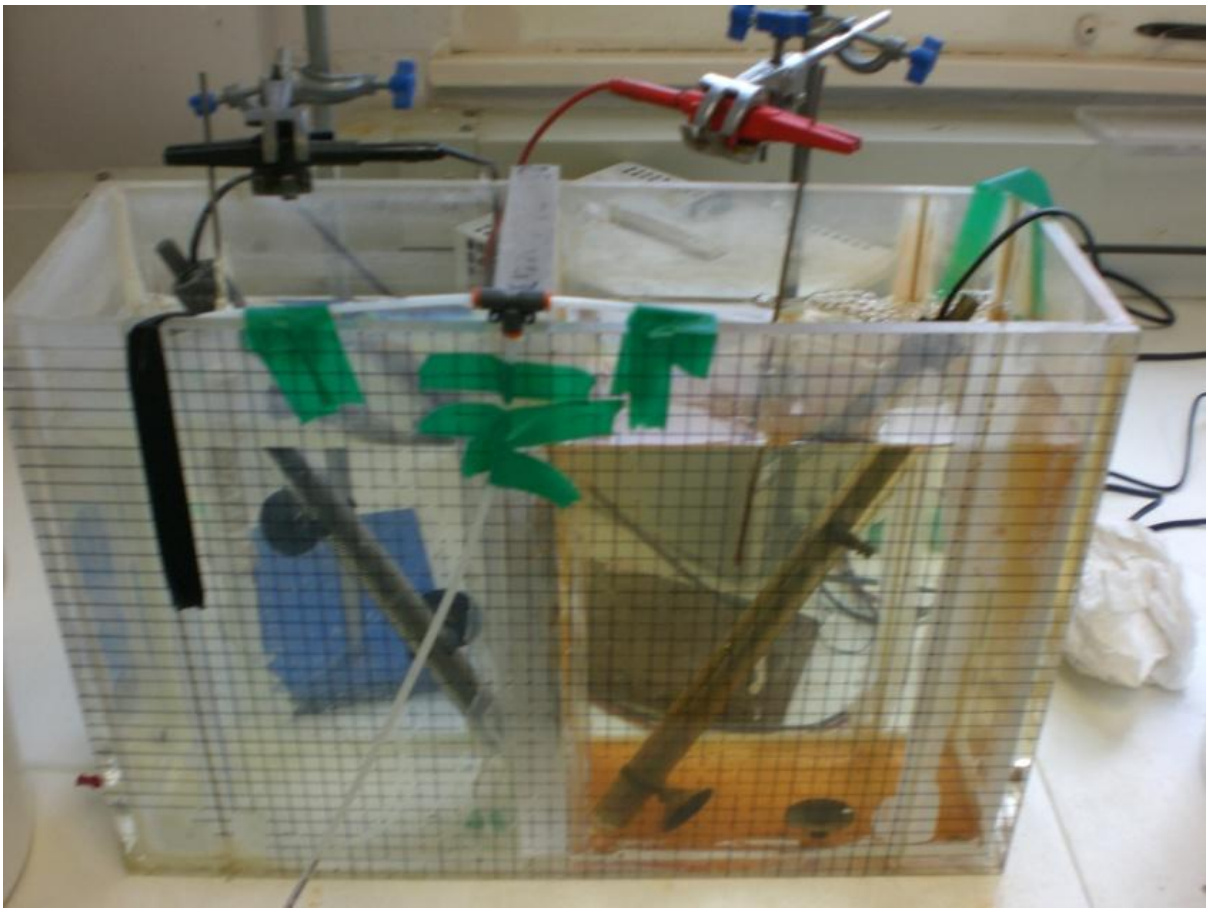

Figure 9.2.5.1 – Set up for LIFTCO2 procedure. Note the cathode compartment on the left and the anode compartment on the right. Aquarium heaters in both compartments. Cathode and Anode electrodes. The CO_2 supply split between both sides with a "T" connector.

Figure 9.2.5.2 (left) and 9.2.5.3 (right). A hammer and nylon rod are used to force the samples out of the Perspex sheet

9.3 Testing of Samples

After the attempts at replicating CO_2 degradation three different tests were undertaken:

- Strength testing to determine the UCS

- Use of the Scanning Electron Microscope (SEM)
- Use of XRD machine

The samples are strength tested using the hydraulic testing machine in the Structures Lab with a loading rate of 2400N/s.

The hydraulic strength testing machine in the structures lab was used for the large samples as this has a higher maximum loading than that in the geotechnical lab whose capacity might be exceeded.

SEM and XRD are both expensive to perform and so the amount of usage allowed was limited and not applied to all samples. Ultimately this allowed 10 samples to be XRD tested and 8 samples to be sent for SEM analysis. Table 9.3.1 shows which samples were tested. It was decided to avoid testing the intermediate mixtures with 3% MgO and prioritise the mixtures with minimum/maximum MgO added as these would be most likely to exhibit the extremes in behaviours.

Table 9.3.1 Tests applied to each sample

	Composition	UCS Tested?	XRD?	SEM?
No degradation – Control	Mixture 1	Yes	Yes	Yes
	Mixture 2	Yes	No	No
	Mixture 3	Yes	Yes	Yes
	CO_2 resistant cement	Yes	Yes	Yes
Degradation Simulation 1	Mixture 1	Yes	Yes	No
	Mixture 2	Yes	No	No
	Mixture 3	Yes	Yes	No
Degradation Simulation 2	Mixture 1	Yes	Yes	Yes
	Mixture 2	Yes	No	No
	Mixture 3	Yes	Yes	Yes
Degradation Simulation 3	Mixture 1	Yes	No	No
	Mixture 2	Yes	No	No
	Mixture 3	Yes	No	No
Degradation Simulation 4 (LIFTCO2 Procedure)	Mixture 1	Yes	Yes (1 for cathode side, 1 for anode side)	Yes (1 for cathode side, 1 for anode side)
	Mixture 2	Yes	No	No
	Mixture 3	Yes	Yes (1 for cathode side, 1 for anode side)	Yes (1 for cathode side, 1 for anode side)
	CO_2 resistant cement	Yes	Yes (1 for cathode side)	Yes (1 for cathode side)

The LIFTCO2 paper suggests chemistry at the anode will be largely different to the cathode. The direction of ion movement due to leaching will depend on which way round the electrodes are connected. Additionally the pH will be different in each compartment due to the forced dissociation of either H^+ or OH^- ions.

Taking account of this the top and bottom ends of these samples are analysed separately for SEM and XRD.

Smooth fragments about a few mm in size were selected as candidates for SEM imaging. It is important that these dry for analysis so the damp samples are wrapped in tin foil then gently heated in the geotechnical lab oven at 120°C for 30 minutes. For the small samples SEM specimens were obtained by sawing off the ends where degradation should be most noticeable. For the large samples the fragments were obtained after testing to destruction (Figure 9.3.1) in the UCS tests. Again smooth samples were taken from the surface where degradation should be most noticeable.

X-Ray Diffraction (XRD) requires the samples to be in powder form. After strength testing the fragments are collected (care is taken to select fragments from the outside of the sample where degradation is most likely to happen first) and crushed using the mechanical grinder. The ground down cement products are then passed through a 75µm sieve. This process is continued until about 10g of sufficiently fine powdered sample has been collected (figure 9.3.2). The samples of each composition mixture are then sent for XRD analysis. For the samples subject to the LIFTCO2 procedure the few mm at the top/bottom end of each sample are taken so powders representative of the anode and cathode sides can be produced.

Figures 9.3.1 (left) – Collecting fragments of sample for SEM analysis (N.B. these would be fragmented further until a few mm in size). Figure 9.3.2 (right) Sample in powder form for XRD analysis.

Given that the CO_2 resistant cement was not received until relatively late on in the project there was a limit to the amount of investigation that could be undertaken. Only small samples were prepared and the only degradation process applied was the LIFTCO2 procedure for 57 days.

The samples were removed with the hammer and nylon rod with a view for strength testing, SEM and XRD analysis.

This took place after the results of XRD and SEM analysis for Mixtures 1-3 had taken place. Bearing in mind the results encountered (to be discussed later) SEM and XRD analysis only took place at the cathode side of the sample to save on time and money.

9.4 Changes to Experimental procedure due to problems encountered

9.4.1 Shrinkage in the Large Samples

During the setting, curing and degradation simulations shrinkage is quite prevalent resulting in many samples having irregular shapes at their ends (Figure 9.4.1.1). This loss of the sample's cylindrical shape could reduce the accuracy of the strength tests if the plates no longer remain parallel to each other during the test causing oblique forces to be applied (Figure 9.4.1.2 - note that this shows a small sample being tested).

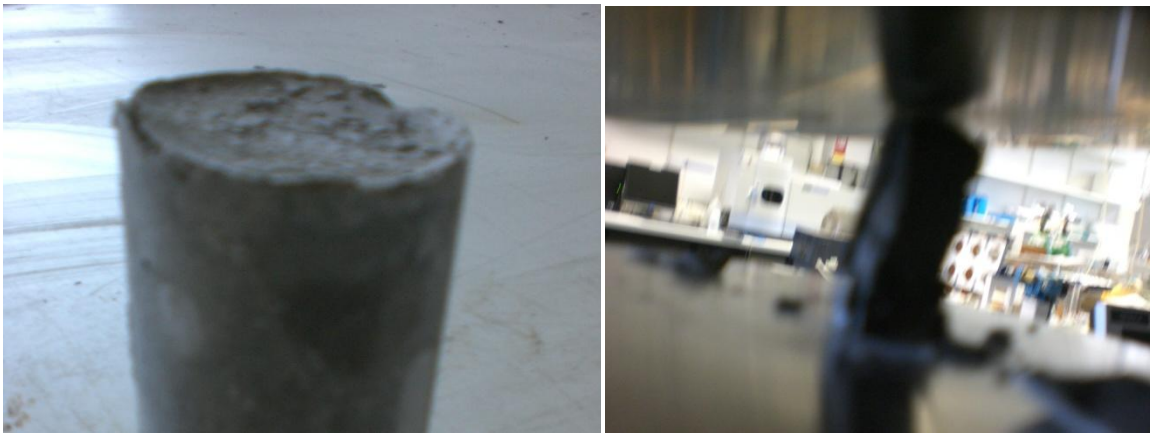

Figure 9.4.1.1 (left): Shrinkage and irregular shaped end in sample. Figure 9.4.1.2 (right): Plates failing to stay parallel to each other when testing an irregular shaped sample.

Standard workshop equipment can be used to remove these irregularities and improve the sample's shape. If the shrinkage and irregularity is small then the protruding edges can simply be chiselled down until both ends of the sample are fairly smooth and even. If lots of shrinkage has occurred then it will be necessary to use the cutting machine in the geotechnical lab. This method of cutting the sample is far from perfect and can dislodge a chunk of the sample upon cutting perhaps giving the sample an even more irregular shape. It

appears cutting the sample at a uniform speed and when damp minimises the amount that this happens.

The amount of shrinkage can vary greatly so the final height of the samples shows some variation. Fortunately about 10 large samples were made for each mixture so there is leeway to discard samples with the most irregular shape and height outside the 93-96mm window.


Figures 9.4.1.3 and 9.4.1.4: Laboratory cutting equipment

9.4.2 Shrinkage in the Small Samples

Shrinkage occurring in the middle of the small samples can cause the small samples to disintegrate upon removal from the Perspex sheet. Even if they can be successfully removed then the reduction in cross-sectional area (perhaps up to about 50%) could severely compromise the accuracy of the strength tests. The fact that the rig provided 13 or 14 of each sample was fortunate as it enabled the 3 most regular sized and shaped samples to be selected for strength testing.

10. Discussion of results

10.1 General observations

For degradation simulations 1-3 there are no noticeable visual signs of degradation though shrinkage is often prevalent and the shape of the samples may change slightly.

After 35 days of the LIFTCO2 procedure the anode compartment water has turned a murky brown colour (Figure 10.1.1). This is likely due to corrosion of the steel electrodes. The cathode electrode has developed a coating of white crystalline solid (Figure 10.1.2). This was

also encountered by Rimmelé and Gouedard whose more detailed analysis found this to be calcite and vaterite. If this is the case then degradation of some sort must have occurred. Distilled water is used so the source of the Calcium ions must have been the cement.

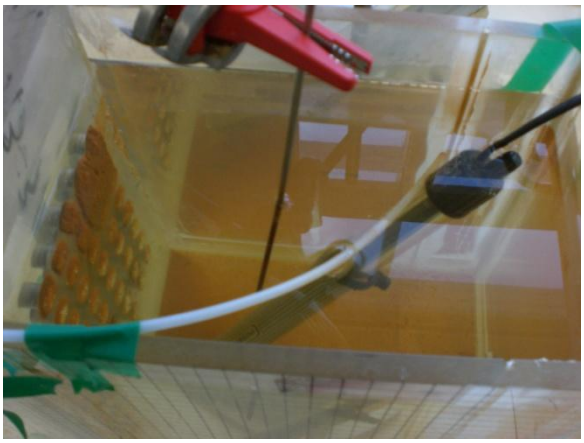


Figure 10.1.1 (left): Anode compartment after 25 days of LIFTCO2 procedure. Figure 10.1.2 (right): White crystalline calcite precipitated on cathode electrode.

The application of an electric potential also drives a pH imbalance across the LIFTCO2 cell (depending on whether H^+ or OH^- ions are favoured). The pHs of the anode and cathode compartments tend to equilibriate at about 4.9 and 6.3 respectively. This acidic environment could influence the rate of degradation at the anode side.

10.2 Strength Test Results, SEM images and XRD Profiles

Having selected the samples with the most similar size and shape the average strength is obtained for each mixture and degradation simulation (more detailed results in Appendix) by dividing the force applied by the cross-sectional area of the sample. These results are presented in Figure 10.2.1 and Table 10.2.1

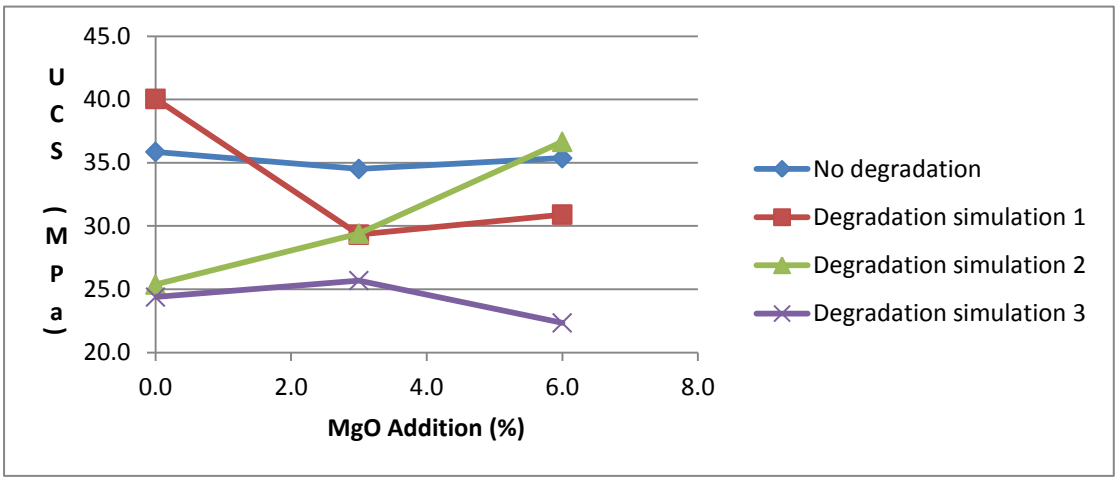

Figure 10.2.1 Effect of MgO addition on UCS for each degradation simulation

It is difficult to draw any overwhelmingly strong conclusions from Figure 10.2.1 and Table 10.2.1. The data suggests MgO has little impact on strength in the control samples.

The degradation simulations appear to have varying degrees of effect. Simulation 3 causes a reduction in strength across all compositions while with Simulations 1 and 2 the effect is less clear. Simulation 1 seems to increase the control sample's strength while Simulation 2 causes it to undergo a noticeable reduction. Simulation 1 suggests a low MgO content is more resistant to degradation while Simulation 2 suggests MgO additive could be beneficial.

Table 10.2.1 Average UCS (MPa) for given composition and degradation simulation

	No degradation	Degradation Simulation 1	Degradation Simulation 2	Degradation Simulation 3
Mixture 1	35.9	40.0	25.4	24.4
Mixture 2	34.5	29.3	29.4	25.7
Mixture 3	35.4	30.9	36.7	22.3

There is admittedly a large amount of deviation in the results and this should be remembered when analysing the results. Standard Deviations as a percentage of the mean for the UCS for each mixture and degradation simulation are highlighted in Table 10.2.2. Given the lack of confidence associated with the strength test data XRD and SEM techniques might be more useful. If changes in chemical composition and microstructure brought about by CO_2 degradation can be observed then these might go some way to explaining the strength test results.

Table 10.2.2 Standard Deviation as a percentage of the mean for the UCS for given composition and degradation simulation

	No degradation	Degradation Simulation 1	Degradation Simulation 2	Degradation Simulation 3
Mixture 1	18.9%	21.4%	19.2%	21.7%
Mixture 2	10.7%	23.7%	26.3%	18.5%
Mixture 3	18.6%	15.9%	17.1%	22.2%

X-Ray Diffraction is a very useful analysis tool as it gives a clear indication as to the chemical compounds present in the cement samples. It can be used for more detailed quantitative analysis (e.g. RIR method) but this is beyond the scope of the 4th year project.

Firstly XRD can be used to suggest the compounds and hydration products present in our simple water and cement mixture. By matching up the peaks on the spectroscopy profile in Figure 10.2.2 with those of common minerals we deduce that Portlandite is the most abundant hydration product with Brucite ($Mg(OH)_2$) present in smaller quantities - recall that the API Class G cement contains 1.8%MgO.

The analysis also indicates the presence of the carbonation product Nesquehonite in a small quantity even in the control sample when no deliberate attempt is made to try to encourage carbonation. Note that across all XRD graphs arbitrary shifts in the y-direction have been applied for ease of viewing.

As an illustrative example, the Spectroscopy profiles of the mixture containing purely water and cement (Mixture 1) and the mixture with 6% reactive MgO (Mixture 3) added can be compared (Figure 10.2.3). The profiles are very similar with the exception of the circled peak at about 43° corresponding to the presence of Periclase (MgO), associated with the addition of 6% MgO.

When analysing the SEM images it is useful to refer to a paper by Liska et al.[10] that contains useful example images of many of the hydration and carbonation products encountered in this project. It also shows their XRD profiles as a useful reference.

The SEM's of Mixtures 1 and 3 not subject to any degradation have been produced in Figures 10.2.12 and 10.2.13 to complement the XRD data. As expected they are very similar. The hexagonal structure of portlandite can be identified in both samples. The addition of MgO has clearly not had a major impact on microstructure here. There is no sign of Periclase (cube and octahedron shaped crystals) in the SEM images.

Given the composition of the cement (contains 57% $(CaO)_3SiO_2$) used we would also expect C-S-H to be abundant as a hydration product. This can't be indentified on the XRD profiles and can exist in gel form so may be responsible for coating the other crystal structures and blurring the SEM images slightly.

The XRD profiles for Mixtures and 1 and 3 subject to degradation simulation 1 are compared to the control in Figure 10.2.4 (note there was insufficient time and funding to produce SEM's here). The difference between the 2 profiles is also plotted. Any chemical changes in hydration or carbonation products should show up here. Both XRD profiles show that there

might be a slight fall in the amount of Portlandite present (difference in peak height at about 18° is circled) though there is no obvious build up of calcites or carbonates which are tell-tale signs of degradation. The differences between the 2 profiles here could easily be due to inhomogeneities in mixing and then taking the XRD analysis of different parts of the sample. As such there is no conclusive evidence that Degradation Simulation 1 has been effective neither is the evidence that the MgO additive has had any effect as the profiles for Mixtures 1 and 3 show a similar pattern (see Figure 10.2.5).

Degradation Simulation 3 seemed to have the biggest impact on the strength test values so both XRD and SEM have been taken here to see if there is a logical explanation for this. Figure 10.2.6 shows the effect of Degradation Simulation 3 on mixtures 1, the control sample. There are slight differences in peak heights again at about 18° (which could correspond to Portlandite) and also at about 29° and 33°, though these differences are very small and don't correspond well to any suggested hydration or carbonation products. The addition of MgO in Mixture 3 causes a similar change in the XRD profile in Figure 10.2.7 so there is no evidence that either the Degradation Simulation has been effective or that MgO has been an effective additive.

The SEM images re-enforce this argument. There don't appear to be any major differences in microstructure as a result of Degradation Simulation 3 and MgO addition (comparing Figures 10.2.14 and 10.2.15). Hexagonal crystals of Portlandite can be seen in both which re-enforce the XRD results. Crucially though there does not appear to be any evidence of products of carbonation such as $CaCO_3$.

It is the analysis of the results of the LIFTCO2 procedure (Degradation Simulation 4) that seem to show most effect of changes in microstructure, chemistry and thus CO_2 degradation.

XRD profiles have been plotted in Figure 10.2.8 for the control sample, the anode and cathode sides of Mixture 1 subject to the LIFTCO2 procedure for 5 weeks.

Attempts have been made to highlight the peaks corresponding to Portlandite and the smaller amounts of Nesquehonite and Brucite that may be present. Clearly there are some differences between the 2 profiles but analysis becomes a lot easier if we work out the change in the profiles relative to the control sample. Thus figure 10.2.9 plots the true effect of the LIFTCO2 procedure on the XRD profiles at the anode and cathode sides.

Figure 10.2.9 shows much more evidence of change at the cathode side. Clearly the main observation is the decrease in peak heights associated with Portlandite and the increase in peak heights associated with either Calcium (Calcite) or Magnesium Carbonates (the peaks are co-incident so more detailed quantitative analysis of the XRD profiles would be required to differentiate the two). The changes at the cathode are very similar to what Rimmelé and Gouedard observed in their accelerated CO_2 degradation experiments. We conclude that the degradation has occurred and the following reaction has taken place:

$Ca(OH)_2 + CO_3^{2-} + 2H^+ = CaCO_3\ (s) + 2H_2O$
Portlandite => Calcite

Closer observation reveals that the peaks possibly associated with Nesquehonite may have decreased slightly. Given the content of Magnesium Carbonates may have increased the LIFTCO2 procedure could potentially be dehyrdrating the Nesquehonite:

$MgCO_3 \cdot 3H_2O\ (s) => MgCO_3 + 3H_2O$

This would need to be confirmed by more detailed quantitative analysis such as the RIR method. The decomposition of Portlandite clearly occurs on a much larger scale. The amount of Nesquehonite present is small compared to the Portlandite as is confirmed by the XRD profiles and SEM imaging.

Figures 10.2.10 and 10.2.11 show the effect of the LIFTCO2 procedure on Mixture 3 with 6% MgO added.

Figure 10.2.11 still shows reduction in the height of peaks associated with Portlandite and increase in those associated with calcite. It suggests that the MgO addition has not caused the Brucite to undergo Carbonation instead of the Portlandite as was hoped. Although the small peaks associated with Calcite build-up are perhaps less obvious a more detailed quantitative analysis would be required to try to determine whether this rate of reaction has been slowed. It is important to remember that for applications in CCS where cement integrity needs to be maintained for thousands of years even low rates of Portlandite carbonation could prove catastrophic as this will eventually lead to amorphous Silica gel formation. Note that there is no evidence of Dypingite or Hydromagnesite being formed in any of the XRD profiles or SEM images.

Figure 10.12.16 shows the presence of many Calcium Carbonate crystals where some hexagonal crystals can still be identified. Figure 10.12.17 is included more for interest than to make a clear point. It appears to show a very localised spot of needle structures present in a small proportion. A likely explanation is that the Portlandite crystals have taken on a different structure owing to non-uniformities in concentrations from imperfect mixing[11].

Figures 10.12.18 and 10.12.19 show different points on a sample of mixture 3 subject to the cathode side of the LIFTCO2 procedure. Figure 10.12.18 appears to show a degradation front (see Section 6 and Figure 6.1) as a result of Carbonation. The right hand side of the image shows Calcite crystals. The darker area on the left could be a layer of amorphous silica gel whereby the remaining C-S-H has undergone Carbonation as follows;

$3H_2CO_3 + Ca_3Si_2O_7*4H_2O \Rightarrow 3CaCO_3 + 2SiO_2*H_2O + 3H_2O$

Having encountered degradation in the LIFTCO2 procedure the strength test results shall now be presented. Note that it is not valid to compare the UCS as a result of Degradation Simulation 4 to the other simulations given they test small and large samples respectively (notice the values are very different) and the LIFTCO2 procedure samples have been aged for a different length of time.

Table 10.2.3: Average UCS for samples subject to LIFTCO2 procedure

	UCS (Mpa)
Mixture 1 (No MgO)	5.17
Mixture 2 (3% MgO)	3.47
Mixture 3 (6% MgO)	2.80

The fall in UCS with increasing MgO content is what might be expected. It appears to offer no improved properties upon carbonation so the fall in strength can be attributed to the fall in proportion of API Class G cement in the sample.

In all the degradation simulations analysed MgO addition only seems to cause an increase in the amount of Periclase present. There are no noticeable increases in Brucite levels as a result of MgO addition. Crucially studies by Liska et al.[6,7] found that MgO addition resulted in Brucite production given their different curing methods. They found that carbonation instigated the conversion of Brucite to Nesquehonite which tended to increase the strength, stiffness and toughness of the cement:

Brucite ($Mg(OH)_2$) + Carbonation ($CO_2 + 2H_2O$) => Nesquehonite ($MgCO_3(H_2O)_3$)

$Mg(OH)_2 + CO_2 + 2H_2O \Rightarrow MgCO_3(H_2O)_3$

The API recommend curing cement samples in water at 60°C for 8-24 hours as an atmospheric pressure simulation (they recommend curing processes at elevated pressures but these were considerably greater than the resources available) of the oil well cementing process, hence the reason for the choice of curing method. Clearly this curing method does not cause Brucite to form as an abundant hydration product (or to be more precise additional MgO does not increase Brucite levels).

If Brucite content is not increased then no additional Nesquehonite, Dypingite or Hydromagnesite can be formed as a result of the aforementioned reaction and the more beneficial microstructure noted by Liska et al. cannot be realised.

As previously mentioned the CO_2 patented cement has a very sandy structure. It is difficult to obtain suitable samples for strength testing as most simply disintegrate when removed from the Perspex sheet with the Nylon rod. Even when 3 of each sample are finally obtained for strength testing the results are extremely variable. The raw data has been deliberately presented here to highlight the amount of variation in the results:

Table 10.2.4: UCS results for CO2 resistant cements subject to LIFTCO2 procedure

	UCS (Mpa)
Control sample 1	1.06
Control sample 2	2.98
Control sample 3	0.95
Degradation sample 1	2.09
Degradation sample 2	0.86
Degradation sample 3	3.23

Clearly these results are inconclusive given their large variation. Although the values for UCS are a lot lower than the Class G cement based samples the patented cement is likely missing many additives which would increase its strength. This should also explain the crumbly structure of the samples.

Figure 10.2.20 plots the effect of the LIFTCO2 procedure on the cathode side of the CO_2 resistant cement. It clearly shows that the chemistry is significantly different with Quartz (SiO_2), Calcite and caustic MgO the main compounds present.

Figure 10.2.21 shows the difference between the sample subject to degradation and control samples.

Clearly the LIFTCO2 procedure has caused the levels of Quartz and Calcite to increase at the expense of a fall in caustic MgO levels. Given there is no Portlandite present any CO_2 degradation mechanism will be different so we cannot associate Calcite build-up as a sign of CO_2 degradation. Note that caustic MgO typically contains additional traces of CaO (typically 2%) and SiO_2 (6%)[12]. This explains the origin of the Calcium and Silicon and why an increase in Quartz and Calcite levels could occur.

Figures 10.2.22 and 10.2.23 compare effect of the LIFTCO2 procedure on the SEM's of the CO_2 resistant cement. A Calcium Carbonate Crystal structure can be seen in both images.

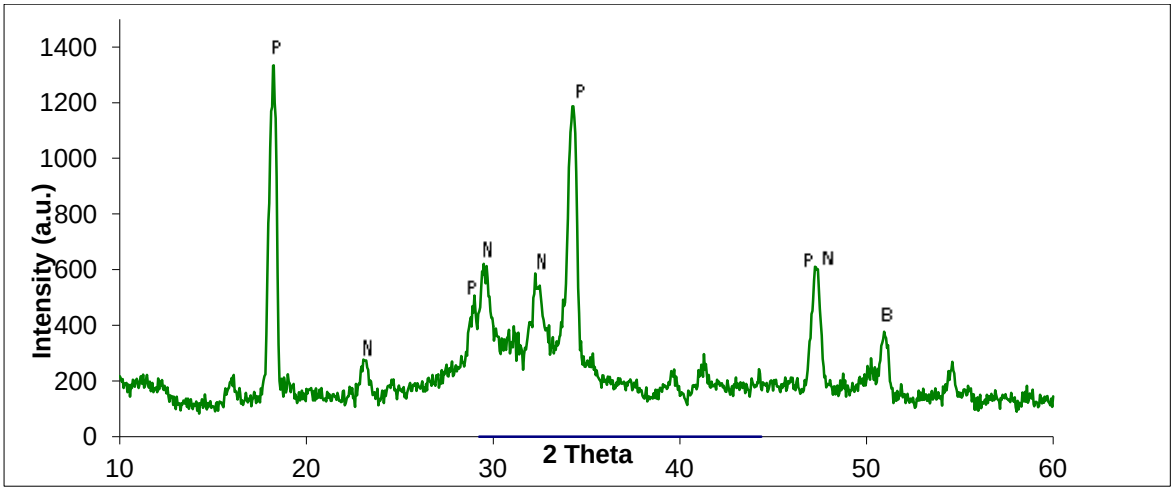

Figure 10.2.2 (above): X-Ray Diffraction Profile for Mixture 1 subject to no degradation: P – Portlandite, B- Brucite, N-Nesquehonite, M – MgO Periclase. Figure 10.2.3 (below) X-Ray Diffraction Profile for Mixtures 1 and 3 subject to no degradation: P – Portlandite, B- Brucite, N-Nesquehonite, M – MgO Periclase

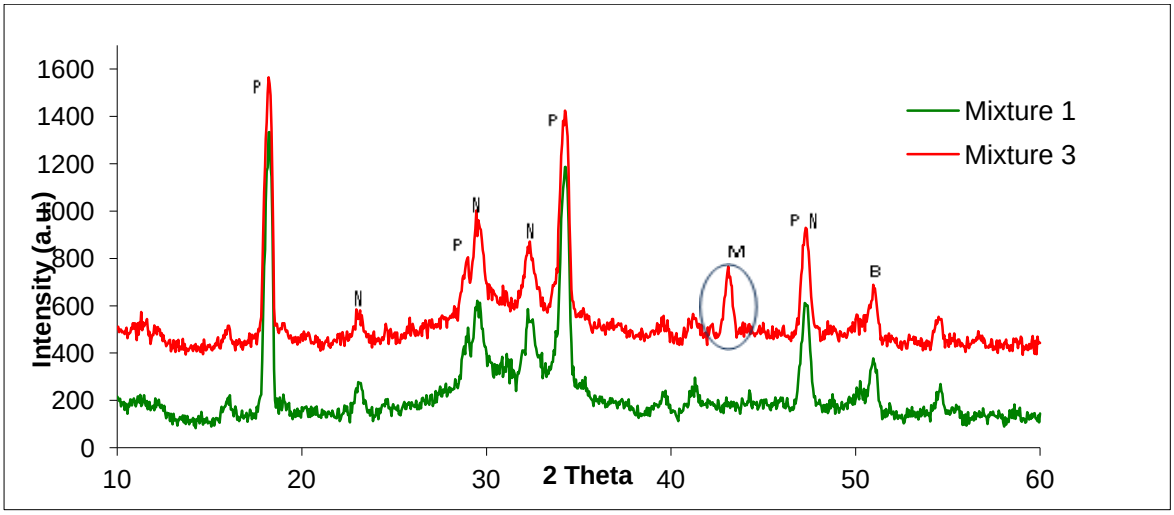

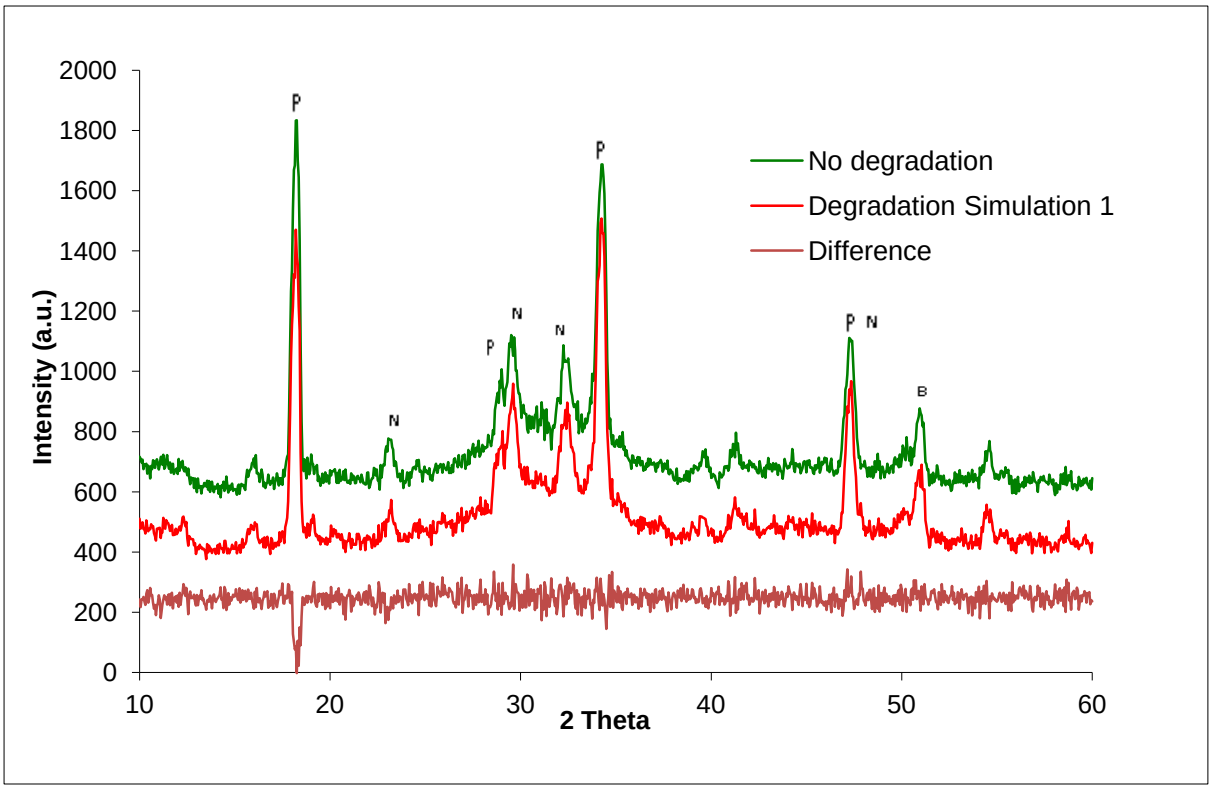

Figure 10.2.4 (above): Effect of degradation simulation 1 on X-Ray Diffraction Profile for Mixture 1: P – Portlandite, B- Bru cite, N-Nesquehonite, M – MgO Periclase.

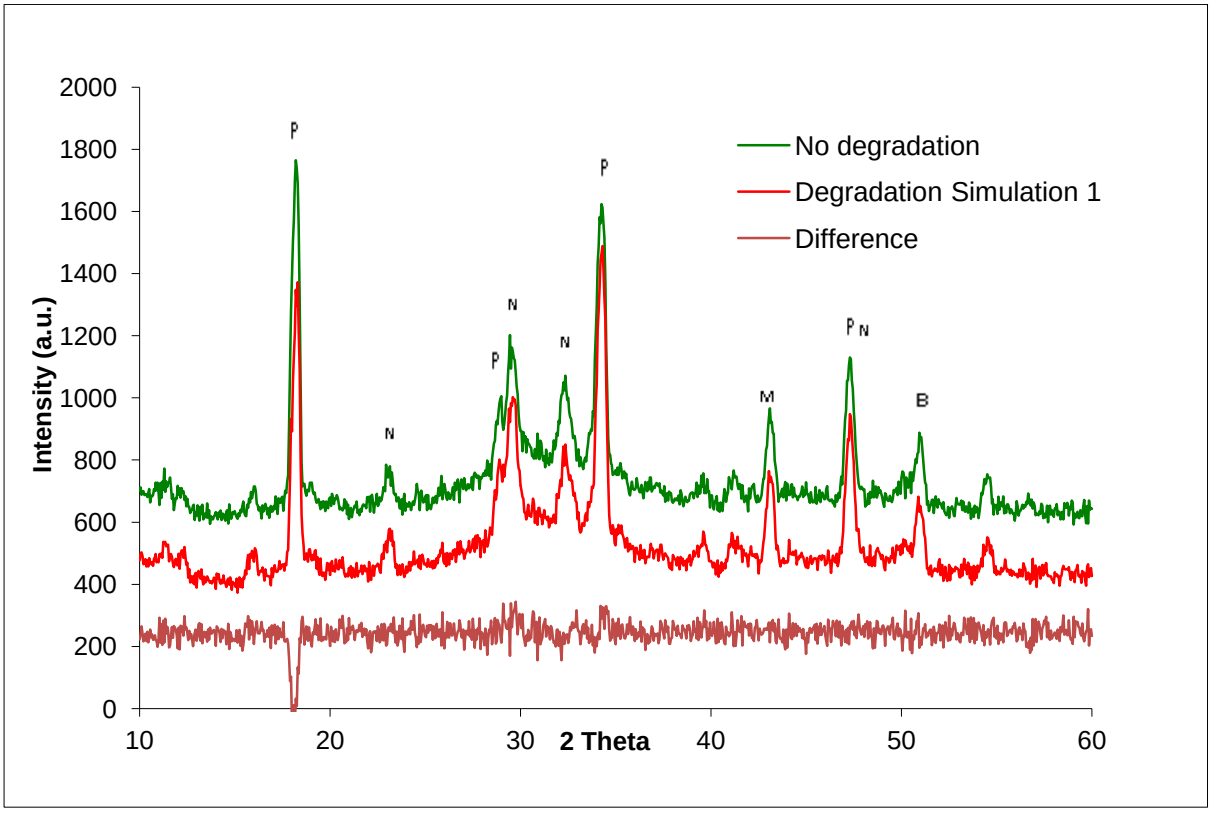

Figure 10.2.5 Effect of degradation simulation 1 on X-Ray Diffraction Profile for Mixture 3: P – Portlandite, B-Brucite, N-Nesquehonite, M – MgO Periclase

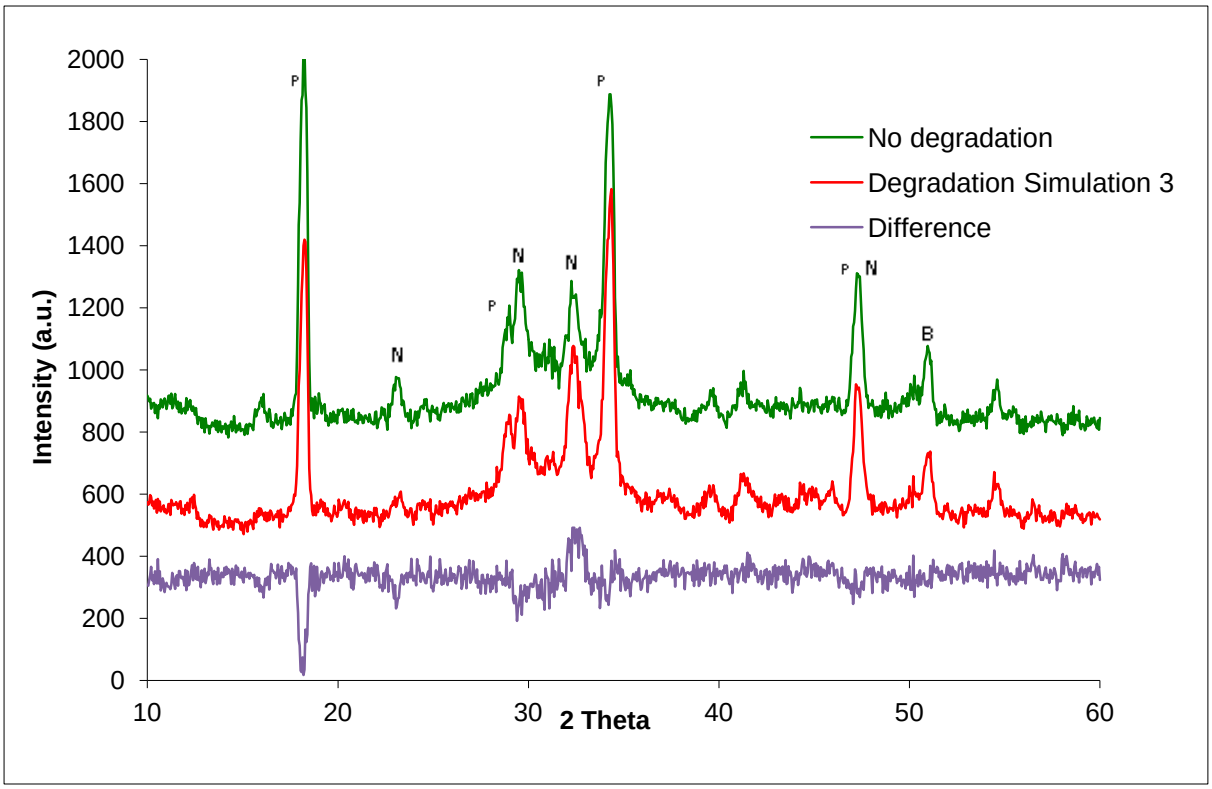

Figure 10.2.6: Effect of degradation simulation 3 on X-Ray Diffraction Profile for Mixture 1: P – Portlandite, B-Brucite, N-Nesquehonite, M – MgO Periclase

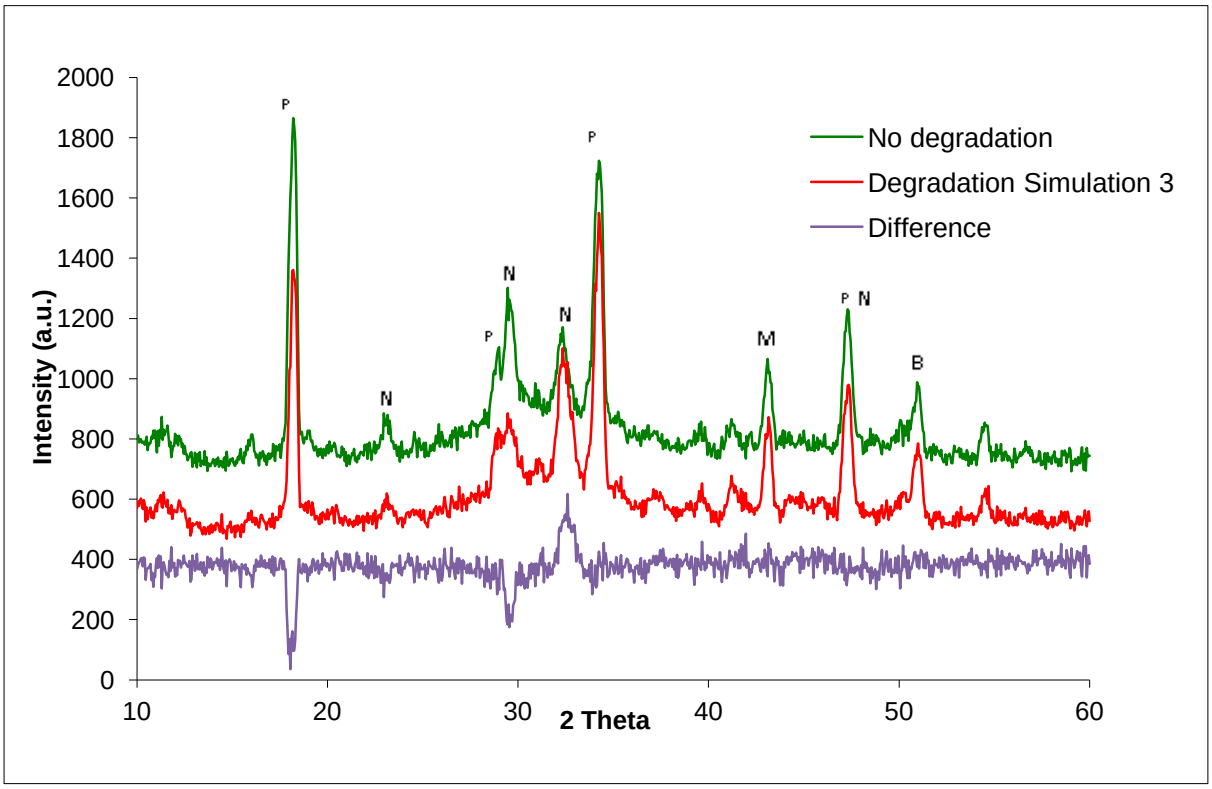

Figure 10.2.7: Effect of degradation simulation 3 on X-Ray Diffraction Profile for Mixture 3: P – Portlandite, B-Brucite, N-Nesquehonite, M – MgO Periclase

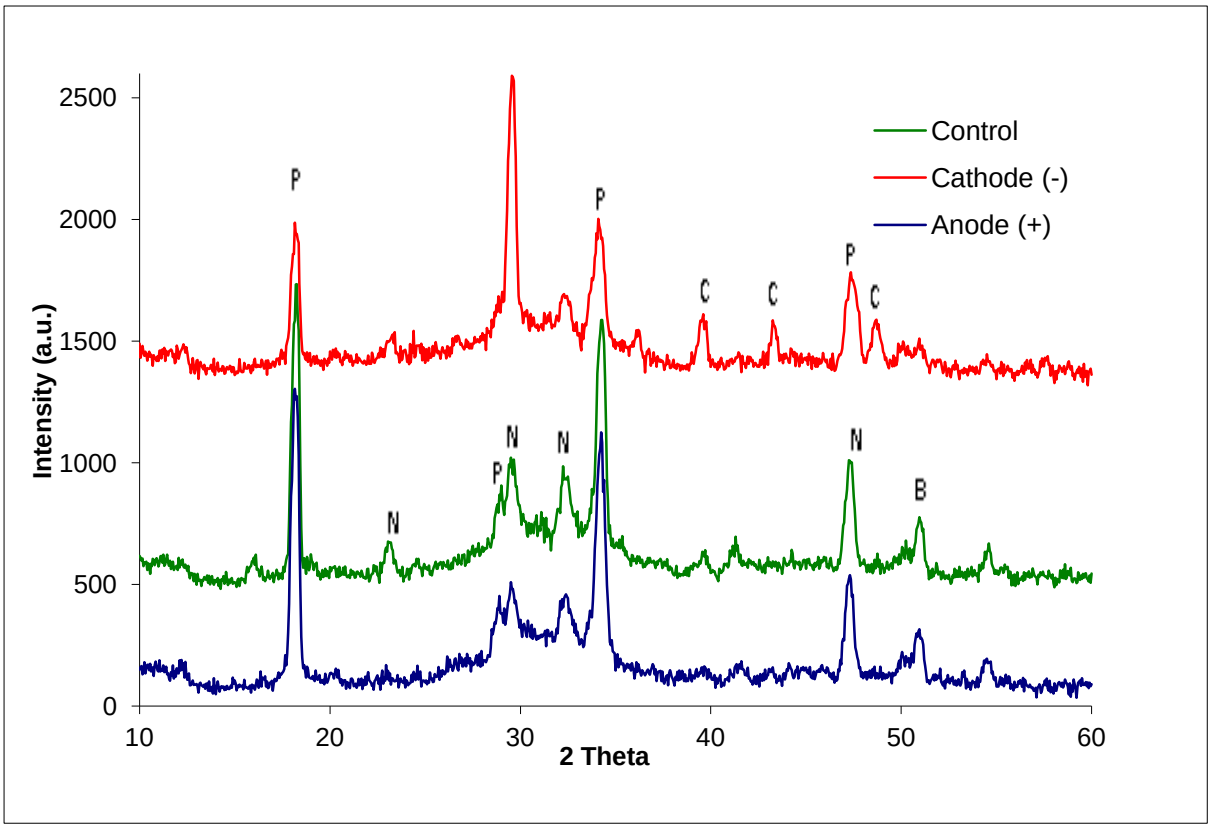

Figure 10.2.8: Effect of LIFTCO2 Procedure (degradation simulation 4) on Anode and Cathode side of mixture 1: P – Portlandite, B- Brucite, N-Nesquehonite, M – MgO Periclase, C – Calcite/Mg or Ca Carbonates

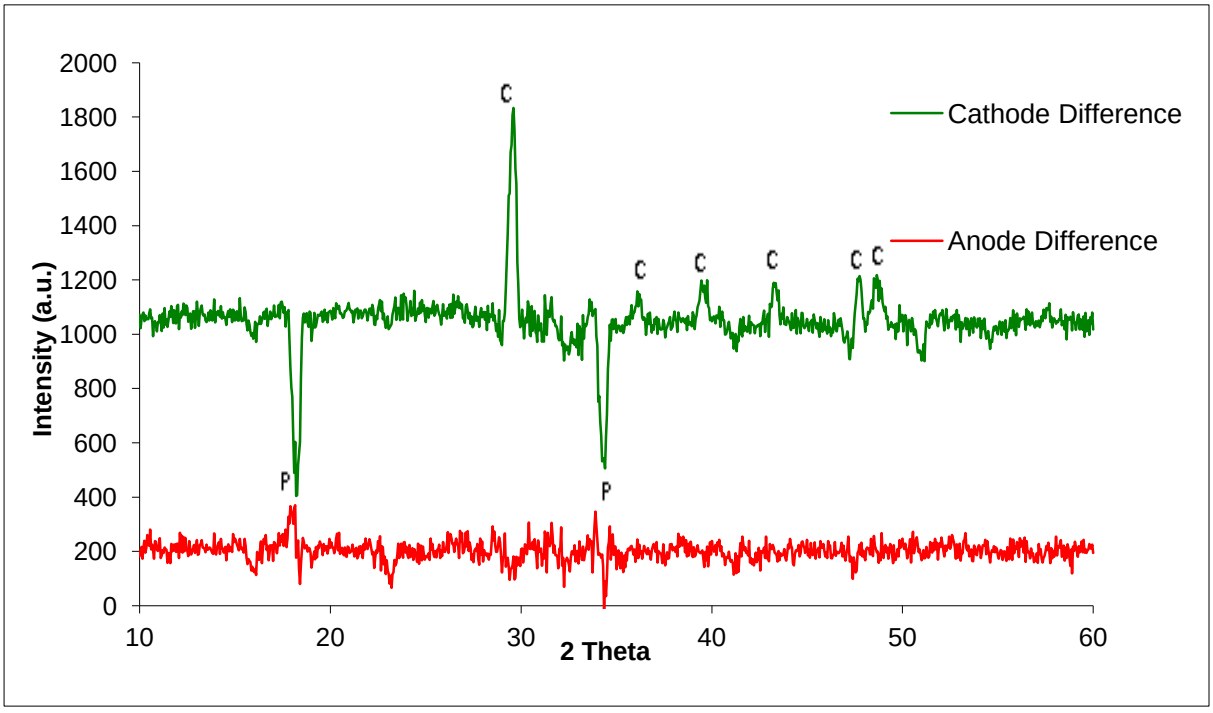

Figure 10.2.9: Difference in XRD profiles (relative to control) for Anode and Cathode side of mixture 1 as a result of LIFTCO2 procedure. P – Portlandite, B- Brucite, N-Nesquehonite, M – MgO Periclase, C – Calcite/Mg or Ca Carbonates

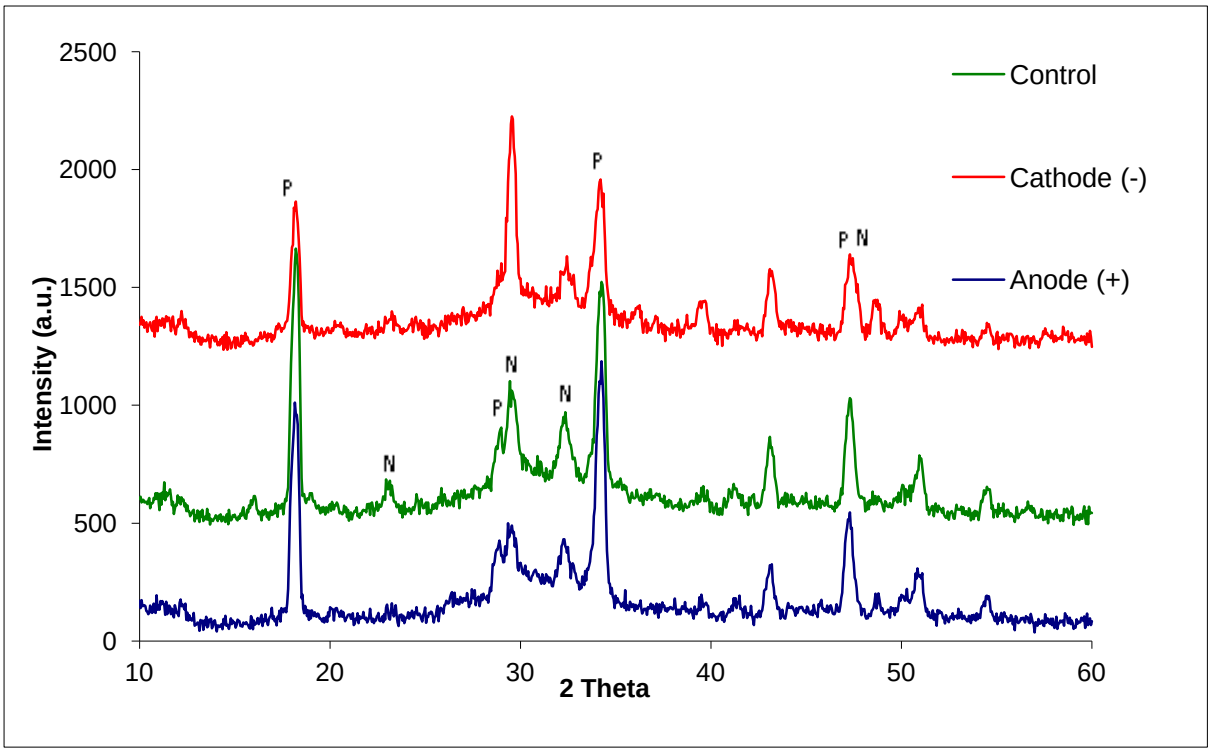

Figure 10.2.10: Effect of LIFTCO2 Procedure (degradation simulation 4) on Anode and Cathode side of mixture 3. P – Portlandite, B- Brucite, N-Nesquehonite, M – MgO Periclase

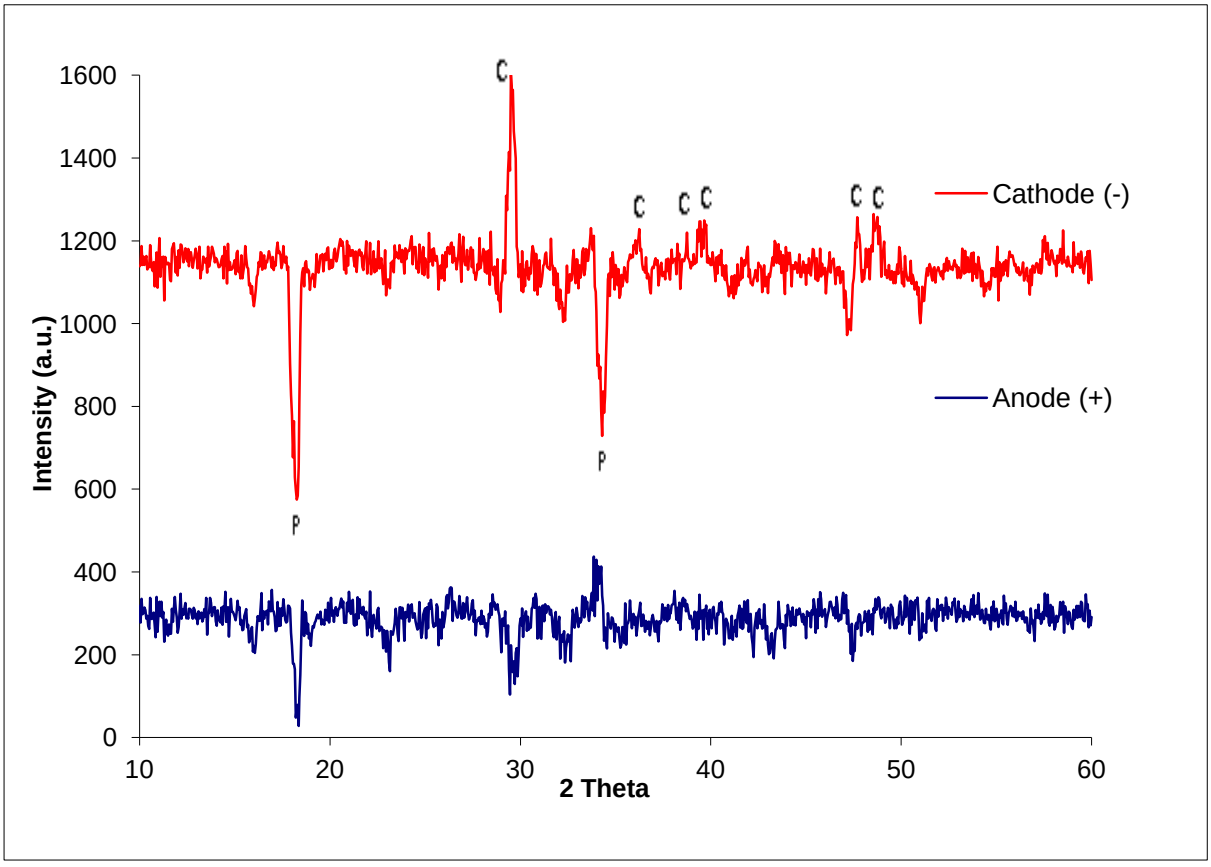

Figure 10.2.11: Difference in XRD profiles (relative to control) for Anode and Cathode side of mixture 3 as a result of LIFTCO2 procedure. P – Portlandite, C – Calcite

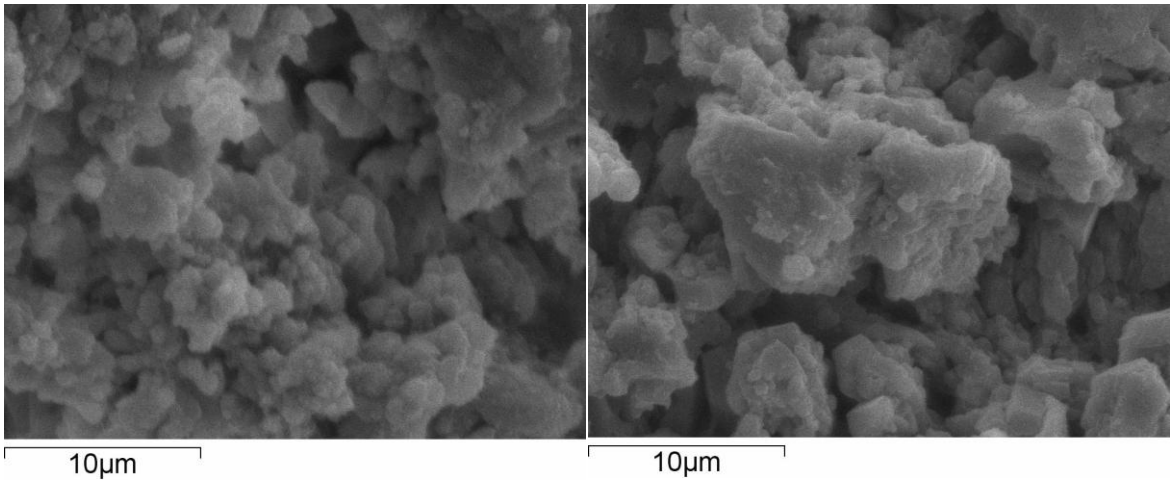

Figure 10.2.12 (left) – SEM for Mixture 1 – No degradation simulated. Figure 10.2.13 (right) – SEM for Mixture 3 – No degradation simulated

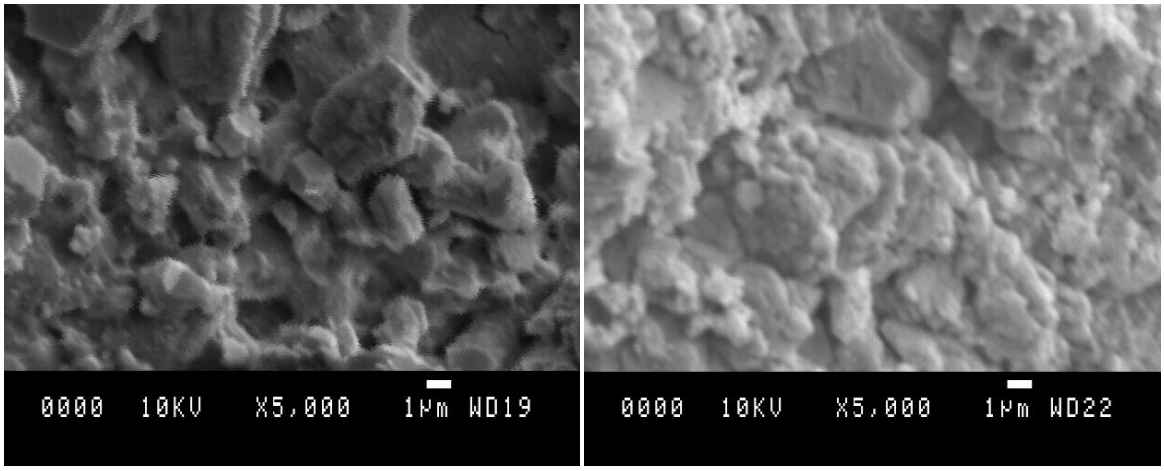

Figure 10.2.14 (left) – SEM for Mixture 1 – Degradation simulation 3

Figure 10.2.15 (right) – SEM for Mixture 3 – Degradation simulation 3

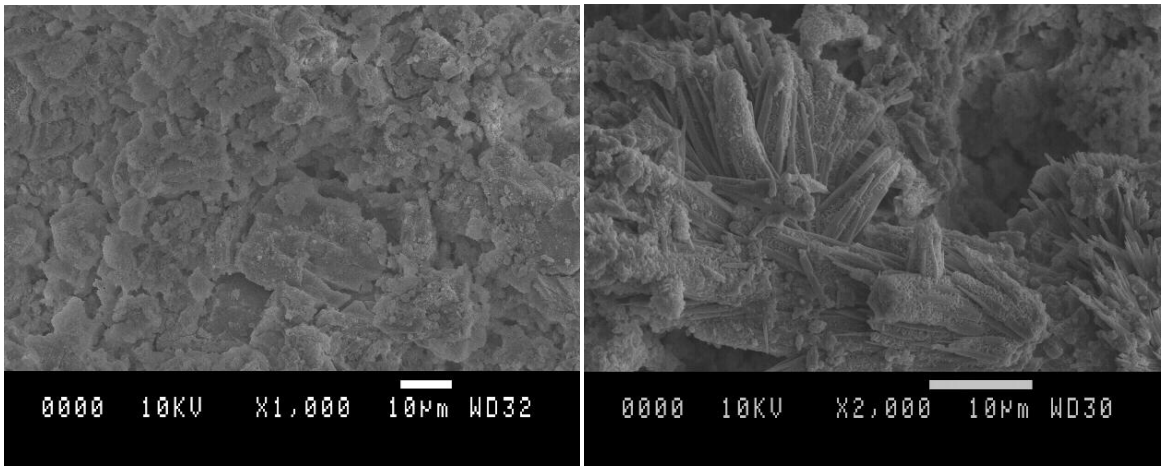

Figure 10.2.16 (left): Cathode side of Mixture 1 after LIFTCO2 procedure. Appears to show mainly Carbonate structure with some Portlandite still evident. Figure 10.2.17 (right): Anode side of mixture 1 subject to LIFTCO2 procedure shows localised spot of ettringite needles and flaky C-S-H crystals on right.

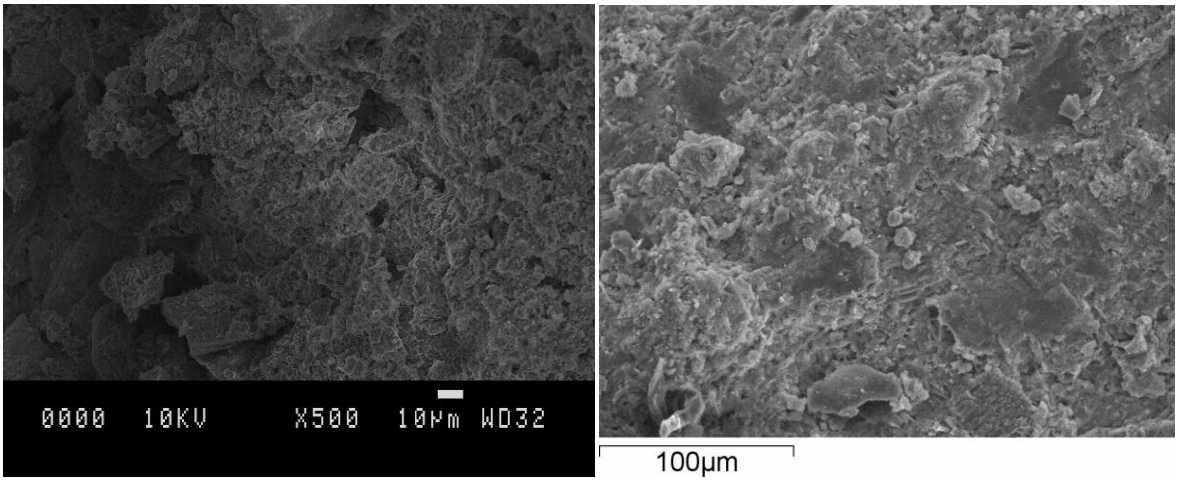

Figure 10.2.18 (left): Cathode side of Mixture 3 after LIFTCO2 procedure showing dark gel layer on left and carbonate structure on right. Figure 10.2.19 (right): Cathode side of Mixture 3 (different location) after LIFTCO2 procedure.

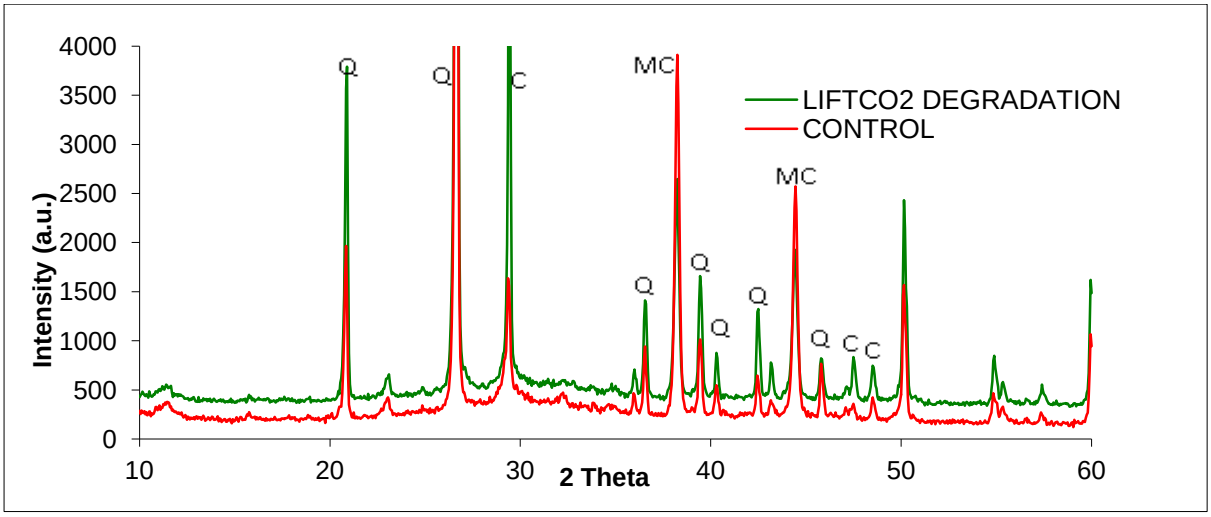

Figure 10.2.20: Effect of LIFTCO2 sample on XRD Profile CO2 resistant Cement. Abbreviations: Q-Quartz, C-Calcite, MC – Caustic MgO

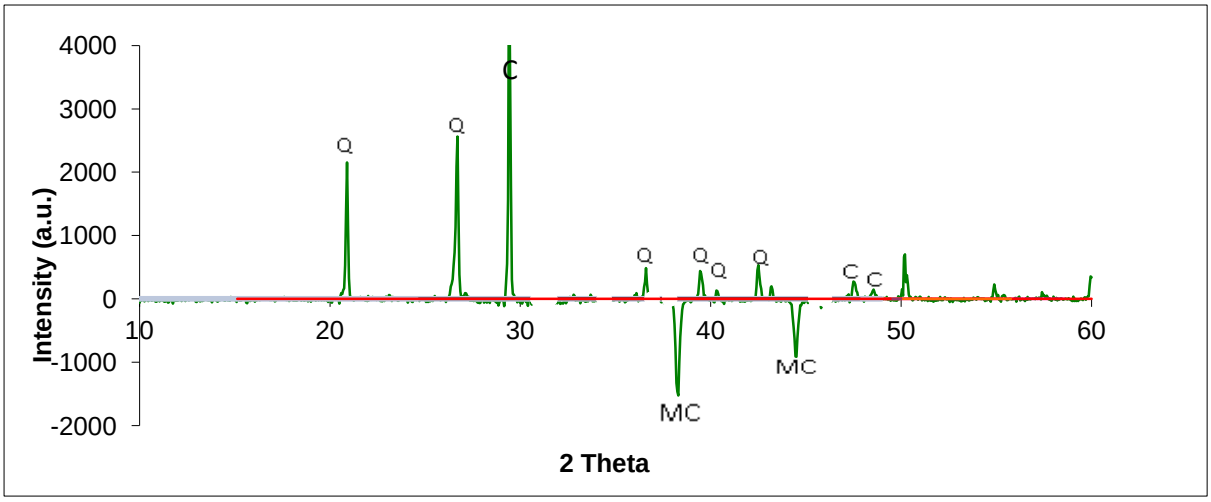

Figure 10.2.21: Difference in XRD Profile of CO2 resistant Cement as a result of LIFTCO2 Procedure. Abbreviations: Q-Quartz, C- Calcite, MC – Caustic MgO

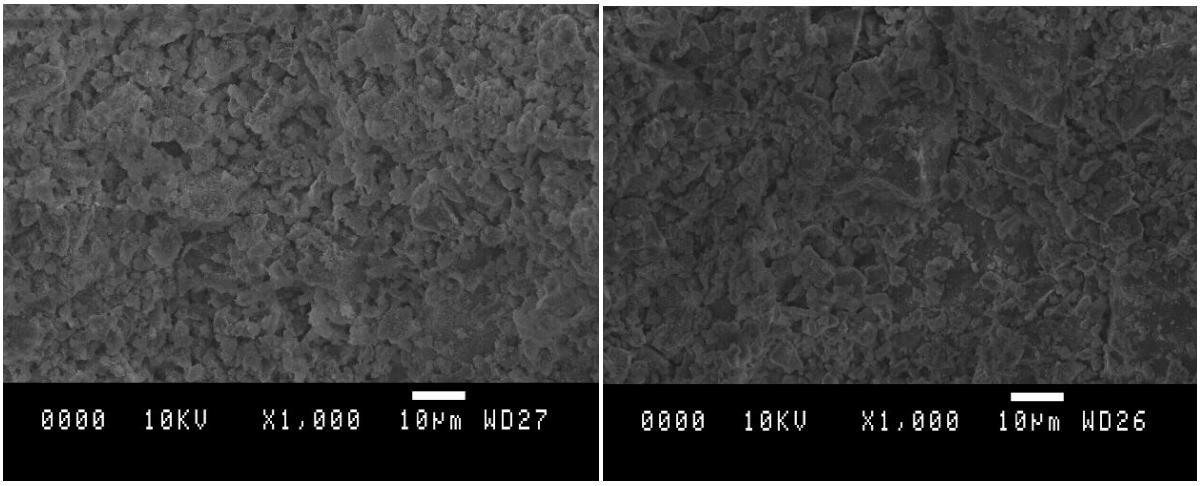

Figure 10.2.22 (left): Control Sample of CO_2 patented cement. Figure 10.2.23 (right): Cathode Side of CO_2 patented cement subject to LIFTCO2 degradation

11. Conclusions

Of the degradation simulations investigated only the LIFTCO2 procedure caused noticeable effects of CO2 degradation; mainly reduced Portlandite and increased Calcite levels hinting that Carbonation has occurred. Some of the SEM images supported this argument.

The samples with extra MgO added did not prevent this carbonation reaction occurring. There was no evidence that the MgO had drastically reduced the rate of carbonation although a more detailed quantitative analysis of the XRD profiles would be needed to determine any quantitative change.

The SEM images and XRD data suggest that Degradation Simulations 1 and 3 have been ineffective at causing Carbonation. Even when degradation has been observed for the LIFTCO2 procedure it occurs over a layer no more than a few hundred µm thick (Figure ??). Thus the volume affected by degradation is very small relative to a large sample so there is no reason to suggest UCS should have changed as a result of these simulations. We therefore put the observed variations and lack of clear trends in UCS down to experimental inaccuracy. There is considerable variation in these results and this could be brought about by:

- Variations in the size and shape of the sample
- Inhomogeneities across samples due to imperfect mixing
- The sample being placed slightly off dead centre in the hydraulic testing machine.

The samples subjected to the LIFTCO2 procedure showed decreasing strength as a result of MgO addition. Given the MgO additive offers no benefit in a CO_2 rich environment the

increase in MgO content implies strength should decrease as the overall proportion of API Class G cement has fallen.

Additional MgO does not increase Brucite levels with the curing method adopted. This means that the cement is unlikely to perform well in a CO_2 rich environment as there is no opportunity for this to be converted to the structurally more favourable carbonation products such as Nesquehonite, Dypingite or Hydromagnesite.

The LIFTCO2 procedure increases the Quartz and Calcite levels of the patented cement.

12. Limitations, Improvements and Future Work

It is important to remember that this study has been highly simplified by not including any additives other than MgO. The API recommended curing process is a sensible method of simulating a well cementing process. There was no evidence that MgO addition increased Brucite levels by way of this curing process and for the cement compositions investigated. A logical follow-up to this investigation would be to see if Brucite formation is more readily encouraged by the use of typical additives alongside the MgO. The range of additives used is vast and likely to be dependent on the environmental conditions. A case study could be done on a specific oil field (preferably one that has been identified as a potential CCS site) and the cement compositions on wells in that area. A "typical" composition might provide a more realistic starting point (and perhaps different results) than our mix of just water and cement.

Clearly the LIFTCO2 procedure has been proven to successfully accelerate the CO_2 degradation process both in this study and that by Rimmelé and Gouedard. It would be wise to use this degradation method in future works.

Adapting the LIFTCO2 rig to increase the sample size would be logical if strength of the cement samples is to be investigated further. Larger samples increase the reliability of subsequent strength tests.

On the other hand if microstructure and chemistry are of more interest, a small sample size is preferable. This serves to increase the proportion of sample affected by the degradation process – important given the degradation front on the sample surface is likely to be less than 1mm thick- and thus make XRD data more representative of the cement that has undergone CO_2 degradation

Cost and health and safety constraints meant we were unable to test samples at high pressures (it turned out no tests were done above atmospheric pressure). Cement used in applications for CCS might have to withstand very high pressures noted in Section 4. The effect of high pressures on CO_2 degradation should be investigated if the opportunity to use a suitable facility arises.

The XRD data obtained has been used in a mainly qualitative manner to try to verify the main hydration products. The RIR method should be considered in future work to deduce accurately proportions in which they are present.

In some cases it might be useful to apply the technique of Electron Diffraction Analysis. Particularly where uncertainty exists about whether Calcium or Magnesium ions are present.

The patented CO_2 resistant cement was not received until the end of March due to administrative delays on behalf of the company involved. Only the cement powder was received and not the additives. If the additives and more detailed information about the cement and additive composition can be obtained then a more informed study could be made about the cement's CO_2 resistance.

13. References/Acknowledgements

*1a) Department of Energy and Climate Change Press Release 3rd April 2011 - http://www.decc.gov.uk/en/content/cms/news/pn12_040/pn12_040.aspx 1) Well Design and Integrity – Wabamun Area CO_2 Sequestration Project – Runar Nygaard. 2) CO_2 for Enhanced Oil Recovery Needs - Enhanced Fiscal Incentives - J Michael Austell. 3) Well Cementing – Schlumberger 4) API Specifications for Oil Well Cementing (Section 10B) – API 5) Degradation of Well Cement by CO_2 under geological sequestration conditions – Kutchko et al. 6) Reactive Magnesium Cements: Properties and Applications – Vandeperre, Liska and Al-Tabbaa 7) Ultra-green construction: Reactive magnesia and masonry products - Liska and Al-Tabbaa 8) Accelerated Degradation method for cement under CO2 rich environment – Rimmelé and Gouédard 9) H2S- CO_2 reaction with hydrated Class H well cement: Acid-gas injection and CO_2 Co-sequestration – Kutchko et al. 10) Production of Magnesia-based masonry. Part 1: Performance – Liska, Al-Tabbaa, Carter and Fifield)11) Images of cement hydration products on www.cementlab.com were useful in the analysis of SEM images. 12) Typical composition from a Caustic MgO supplier -http://www.shouximeiye.com/cgi/search-en.cgi?f=product_en_1_+company_en_1_&id=82491&t=product_en_1_*

13) Cullity B.D. and Stock S.R. Elements of X-RayDiffraction, Powder Technology, Pearson 2003

A technical milestone report was produced summarising the work done in Michaelmas term. This consisted mainly of literature reviews and preliminary experiments. None of the results are deemed worthy of presentation in this report.

I didn't have the necessary training to do the SEM and XRD analysis so thanks go to Fei Jin for doing this on my behalf.

Thanks also go to Cebo UK for providing 100kg of API Class G Oilwell cement free of charge.

Finally thanks go to Dr Abir Al-Tabbaa for supervising me and providing helpful suggestions and ideas along the way.

Appendix 1 – Retrospective Risk Assessment

The risk assessment submitted to the safety officer in October covers all Health and Safety issues fairly effectively. The additional points are raised in retrospect:

- CO_2 patented cement has similar safety procedures to API Class G Cement. Mask, lab coat and rubber gloves must be worn. The dust has been shown to be carcinogenic. The safety officer was consulted about this and provided a properly fitting respirator.
- A Stanley knife used to cut sellotape and clingfilm portions when fabricating the moulds. Presents relatively little risk if used properly.
- The MgO additive used has no major hazards. It is a mild irritant to the eyes and skin. It should not be inhaled. The same procedures about wearing gloves, a mask and a lab coat apply.
- The hydraulic testing machines were used to test the UCS of the cement samples. Retrospectively much attention should be made about the need to wear goggles and ensure there are no bystanders in the area. The fragments can break off the tested cement samples unpredictably and at speed.
- When the risk assessment was submitted it was not anticipated that XRD and SEM would be used. The samples were prepared using a grinding machine. Care should be taken to keep hands and fingers away from moving parts. A respirator was worn to prevent inhalation of the fine powdered dust produced. Fei Jin (PhD Student in Division D) undertook the tests on my behalf while following correct laboratory procedures.
- Mixing of cement samples took place with a bench scale food mixer. The risk associated with this piece of equipment is low but hands and fingers should be kept away from moving parts.
- Some experiments used the stress lab oven for high-temperature testing. A separate risk assessment was submitted for this mainly making sure that the samples had at least 2 hours to cool before being removed with thick oven gloves.
- It was not anticipated that cement samples would undergo shrinkage and require cutting into regular shapes. The geotechnical lab mechanical saw was used. Ear defenders, a respirator and goggles were all worn. Chris Knights, the geotechnical lab technician, demonstrated the safe use of the machine.

Appendix 2 – Data Sheet for API Class G Oil Well Cement Used

Certificate of analysis

CCB
Italcementi Group
Grand-Route 260
B - 7530 Gaurain-Ramecroix
Tel 32 (69)25 25 11
Fax 32 (69)25 25 90

APPROVED
SIGNED
DATE 4/10/11
5/10/11

CEMOIL

API Class G HSR

Customer : CEBO UK			
Laboratory's N° :	82686	Test Report N° :	4.68/11/09/171
Customer PO N° :	1206939	Dated :	September 07, 2011
Quantity :	900.300 Tons in bulk	To	ABERDEEN / UK
Shipped by :	M/S " Ristske "	On :	September 19, 2011

Physical Performance (44% BWOC mix water)		Actual Results	API Spec 10A Requirements
Fineness Blaine	m^2/kg	313	NR
Free fluid	%	4.7	Max. 5.9
Slurry density	lb/gal (kg/l)	15.9 (1.91)	NR
Thickening Time (Depth: 8000ft, BHCT: 52°C)		Test condition: API Schedule 5	
Consistency after 30min	Bc	10	Max. 30
Time to 30Bc	min	80	Min. 30
Time to 100Bc	min	99	Min. 90 /Max. 120
Compressive Strength		Test conditions: W/C 0.44, curing Time 8h, Atmospheric Pressure	
Curing Temp. 100°F (38°C)	MPa	6.3	Min. 2.1
Curing Temp. 140°F (60°C)	MPa	14.1	Min. 10.3

Chemical Composition		Actual Results	API Spec 10A Requirements
Magnesium oxide (MgO)	%	1.8	Max. 6.0
Sulfur trioxide (SO_3)	%	2.6	Max. 3.0
Loss on Ignition	%	0.6	Max. 3.0
Insoluble residue	%	0.12	Max. 0.75
C_3A	%	2.2	Max 3.0
$C_4AF + 2\ C_3A$	%	17.3	Max. 24.0
C_3S	%	57.0	Min. 48.0 /Max. 65.0
$(0{,}658 \times K_2O) + Na_2O$	%	0.47	Max 0.75

Lhassane OUNEJAR
Chef de Service Qualité
et Laboratoire Ciments

E. DERYCKE
Responsable Développement
Qualité-Environnement

Date : September 22, 2011

Appendix 3 – Raw data used for strength test results (excludes samples of unsuitable size/shape)

		Sample number	Failure Strength (kN)	UCS (Mpa)
Control	Mixture 1	8	86.18	43.89
Control	Mixture 1	6	57.21	29.14
Control	Mixture 1	14	82.67	42.10
Control	Mixture 1	1	59.45	30.28
Control	Mixture 1	11	66.52	33.88
Control	Mixture 2	8	76.52	38.97
Control	Mixture 2	1	76.09	38.75
Control	Mixture 2	12	62.19	31.67
Control	Mixture 2	4	65.68	33.45
Control	Mixture 2	2	64.44	32.82
Control	Mixture 2	14	57.56	29.32
Control	Mixture 2	3	71.8	36.57
Control	Mixture 3	13	89.1	45.38
Control	Mixture 3	1	46.92	23.90
Control	Mixture 3	2	64.68	32.94
Control	Mixture 3	6	68.51	34.89
Control	Mixture 3	5	76.04	38.73
Control	Mixture 3	8	66.03	33.63
Control	Mixture 3	4	74.75	38.07
Degradation Simulation 1	Mixture 1	9	86.2	43.90
Degradation Simulation 1	Mixture 1	12	103.38	52.65
Degradation Simulation 1	Mixture 1	7	76.22	38.82
Degradation Simulation 1	Mixture 1	3	68.14	34.70
Degradation Simulation 1	Mixture 1	1	83.95	42.76
Degradation Simulation 1	Mixture 1	4	78.65	40.06
Degradation Simulation 1	Mixture 1	2	38.94	19.83
Degradation Simulation 1	Mixture 1	8	96.9	49.35
Degradation Simulation 1	Mixture 1	10	64.19	32.69
Degradation Simulation 1	Mixture 1	6	87.25	44.44
Degradation Simulation 1	Mixture 1	11	72.66	37.01
Degradation Simulation 1	Mixture 1	5	87.08	44.35
Degradation Simulation 1	Mixture 2	6	41.5	21.14
Degradation Simulation 1	Mixture 2	14	63.45	32.31
Degradation Simulation 1	Mixture 2	12	68.93	35.11
Degradation Simulation 1	Mixture 2	3	74	37.69
Degradation Simulation 1	Mixture 2	4	34.26	17.45
Degradation Simulation 1	Mixture 2	2	37.84	19.27
Degradation Simulation 1	Mixture 2	5	65.92	33.57
Degradation Simulation 1	Mixture 2	9	63.38	32.28
Degradation Simulation 1	Mixture 2	1	60.68	30.90

Degradation Simulation 1	Mixture 2	11	54.89	27.96
Degradation Simulation 1	Mixture 2	2	68.34	34.81
Degradation Simulation 1	Mixture 3	12	61.88	31.52
Degradation Simulation 1	Mixture 3	5	59.33	30.22
Degradation Simulation 1	Mixture 3	2	70.67	35.99
Degradation Simulation 1	Mixture 3	11	64.4	32.80
Degradation Simulation 1	Mixture 3	3	70.79	36.05
Degradation Simulation 1	Mixture 3	1	61.43	31.29
Degradation Simulation 1	Mixture 3	4	63.27	32.22
Degradation Simulation 1	Mixture 3	9	44.12	22.47
Degradation Simulation 1	Mixture 3	14	73.41	37.39
Degradation Simulation 1	Mixture 3	7	64.54	32.87
Degradation Simulation 1	Mixture 3	8	46.15	23.50
Degradation Simulation 1	Mixture 3	10	45.7	23.27
Degradation Simulation 1	Mixture 3	13	63.13	32.15
Degradation Simulation 2	Mixture 1	2	61.14	31.14
Degradation Simulation 2	Mixture 1	1	50.87	25.91
Degradation Simulation 2	Mixture 1	3	49.5	25.21
Degradation Simulation 2	Mixture 1	4	37.78	19.24
Degradation Simulation 2	Mixture 2	1	49.5	25.21
Degradation Simulation 2	Mixture 2	3	36.93	18.81
Degradation Simulation 2	Mixture 2	5	65.67	33.45
Degradation Simulation 2	Mixture 2	2	76.53	38.98
Degradation Simulation 2	Mixture 2	4	59.97	30.54
Degradation Simulation 2	Mixture 3	6	57.43	29.25
Degradation Simulation 2	Mixture 3	5	69.65	35.47
Degradation Simulation 2	Mixture 3	1	92.93	47.33
Degradation Simulation 2	Mixture 3	4	68.2	34.73
Degradation Simulation 2	Mixture 3	2	78.52	39.99
Degradation Simulation 2	Mixture 3	5	65.07	33.14
Degradation Simulation 3	Mixture 1	3	38.31	19.51
Degradation Simulation 3	Mixture 1	2	54.91	27.97
Degradation Simulation 3	Mixture 1	4	63.64	32.41
Degradation Simulation 3	Mixture 1	6	48.56	24.73
Degradation Simulation 3	Mixture 1	1	35.9	18.28
Degradation Simulation 3	Mixture 1	5	45.91	23.38
Degradation Simulation 3	Mixture 2	3	53.22	27.10
Degradation Simulation 3	Mixture 2	1	62.75	31.96
Degradation Simulation 3	Mixture 2	6	49.99	25.46
Degradation Simulation 3	Mixture 2	5	41.13	20.95
Degradation Simulation 3	Mixture 2	4	57.16	29.11
Degradation Simulation 3	Mixture 2	2	38.38	19.55
Degradation Simulation 3	Mixture 3	9	47.95	24.42
Degradation Simulation 3	Mixture 3	3	32.15	16.37
Degradation Simulation 3	Mixture 3	1	47.34	24.11
Degradation Simulation 3	Mixture 3	8	34.89	17.77

Degradation Simulation 3	Mixture 3	6	49.11	25.01
Degradation Simulation 3	Mixture 3	2	38.51	19.61
Degradation Simulation 3	Mixture 3	4	54.16	27.58
Degradation Simulation 3	Mixture 3	5	32.19	16.39
Degradation Simulation 3	Mixture 3	7	58.51	29.80
LIFTCO2 Procedure	Mixture 1	1	394	3.21
LIFTCO2 Procedure	Mixture 1	2	1059	8.63
LIFTCO2 Procedure	Mixture 1	3	450	3.67
LIFTCO2 Procedure	Mixture 2	1	498	4.06
LIFTCO2 Procedure	Mixture 2	2	232	1.89
LIFTCO2 Procedure	Mixture 2	3	548	4.47
LIFTCO2 Procedure	Mixture 3	1	100	0.81
LIFTCO2 Procedure	Mixture 3	2	364	2.97
LIFTCO2 Procedure	Mixture 3	3	568	4.63